Received: 24 February 2019 | Revised: 24 September 2019 | Accepted: 27 September 2019

DOI: 10.1002/mbo3.948

ORIGINAL ARTICLE

MicrobiologyOpen Open Access WILEY

Aspergillus niger upregulated glycerolipid metabolism and ethanol utilization pathway under ethanol stress

Nawaporn Vinayavekhin[1,2] | Wimonsiri Kongchai[1] | Jittra Piapukiew[2,3] | Warinthorn Chavasiri[1]

[1]Center of Excellence in Natural Products Chemistry, Department of Chemistry, Faculty of Science, Chulalongkorn University, Bangkok, Thailand

[2]Biocatalyst and Environmental Biotechnology Research Unit, Faculty of Science, Chulalongkorn University, Bangkok, Thailand

[3]Department of Botany, Faculty of Science, Chulalongkorn University, Bangkok, Thailand

Correspondence
Nawaporn Vinayavekhin, Department of Chemistry, Faculty of Science, Chulalongkorn University, Bangkok 10330, Thailand.
Email: nawaporn.v@chula.ac.th

Funding information
Thailand Research Fund, Grant/Award Number: MRG6180002; Office of the Higher Education Commission, Thailand

Abstract

The knowledge of how *Aspergillus niger* responds to ethanol can lead to the design of strains with enhanced ethanol tolerance to be utilized in numerous industrial bioprocesses. However, the current understanding about the response mechanisms of *A. niger* toward ethanol stress remains quite limited. Here, we first applied a cell growth assay to test the ethanol tolerance of *A. niger* strain ES4, which was isolated from the wall near a chimney of an ethanol tank of a petroleum company, and found that it was capable of growing in 5% (v/v) ethanol to 30% of the ethanol-free control level. Subsequently, the metabolic responses of this strain toward ethanol were investigated using untargeted metabolomics, which revealed the elevated levels of triacylglycerol (TAG) in the extracellular components, and of diacylglycerol, TAG, and hydroxy-TAG in the intracellular components. Lastly, stable isotope labeling mass spectrometry with ethanol-d_6 showed altered isotopic patterns of molecular ions of lipids in the ethanol-d_6 samples, compared with the nonlabeled ethanol controls, suggesting the ability of *A. niger* ES4 to utilize ethanol as a carbon source. Together, the studies revealed the upregulation of glycerolipid metabolism and ethanol utilization pathway as novel response mechanisms of *A. niger* ES4 toward ethanol stress, thereby underlining the utility of untargeted metabolomics and the overall approaches as tools for elucidating new biological insights.

KEYWORDS

Aspergillus niger, ethanol response, ethanol utilization pathway, glycerolipid metabolism, metabolomics

1 | INTRODUCTION

Organic solvent-tolerant microbes play key roles in many industrial bioprocesses, such as biofuel production, biocatalysis, and bioremediation (Nicolaou, Gaida, & Papoutsakis, 2010). To obtain strains with tolerance to these solvents, an approach involves genetically engineering selected strains based on the knowledge of organic solvent-induced stresses and responses (Taylor, Tuffin, Burton, Eley, & Cowan, 2008; Torres, Pandey, & Castro, 2011), which include repression or activation of sporulation (Bohin, Rigomier, & Schaeffer, 1976), induction of stress proteins (Petersohn et al., 2001), biodegradation or secretion of toxic organic solvents (Aono, Tsukagoshi, & Yamamoto, 1998; Bustard, Whiting, Cowan, & Wright, 2002), alteration in cell morphology (Neumann et al., 2005), and adaptation of the cell surface and cell membrane (Aono & Kobayashi, 1997; Weber & de Bont, 1996). Because these responses might be triggered to

counteract chemical toxins, the elevation in their levels might lead to the development of tolerance traits in these microorganisms (Kajiwara et al., 1996; Kang et al., 2007; Mahipant, Paemanee, Roytrakul, Kato, & Vangnai, 2017; Vinayavekhin & Vangnai, 2018).

Aspergillus niger is a filamentous ascomycete fungus, which can be found in almost every environment. It is known as the black mold on rotting fruits and vegetables. Yet, despite these common views of *A. niger* as an undesirable contaminant, it rarely causes disease in humans (Person, Chudgar, Norton, Tong, & Stout, 2010). In fact, it has the GRAS (generally regarded as safe) status for many of its processes (Frisvad et al., 2011) and is one of the most economically useful fungi in the biotechnological industry (Pel et al., 2007). It has been applied in the fermentation process for the production of organic acids, such as gluconic (Ramachandran, Fontanille, Pandey, & Larroche, 2008) and citric acids, with production of the latter exceeding one million metric tons annually (Baker, 2006), and of various extracellular enzymes, including α-amylase or β-glucosidase (Pariza & Cook, 2010). Apart from these industrial usages, *A. niger* has also been utilized in bioremediation processes (Coulibaly, Naveau, & Agathos, 2002; Srivastava & Thakur, 2006), as heterologous hosts for proteins and secondary metabolites production (Lubertozzi & Keasling, 2009) and as a cofermentation partner with *Saccharomyces cerevisiae* for the simultaneous saccharification and fermentation in bioethanol production (Izmirlioglu & Demirci, 2017). The further studies and usages of *A. niger* have also been facilitated by the availability of the genome sequence of three different *A. niger* strains (NRRL3, ATCC1015, and CBS513.88) (Baker, 2006; Pel et al., 2007).

Recently, one of the black spots found on the roof and outside upper wall of an ethanol tank of a petroleum company was investigated and identified as a living organism, *A. niger* strain ES4. The black spots could be found most densely near the valved chimney of the tank where ethanol was allowed to evaporate, which indicated the preference of this strain of *A. niger* for ethanol. This finding was rather surprising, as most non-ethanol-producing species are not capable of tolerating a high concentration of ethanol.

Relating to ethanol tolerance, *A. niger* isolated from spoiled pastry products was shown previously to be able to grow on potato dextrose agar containing ethanol up to about 3% (*w*/*w*) with almost no growth defect and up to 4% (*w*/*w*) with about 50% reduction in its growth (Dantigny, Guilmart, Radoi, Bensoussan, & Zwietering, 2005). Another unrelated study also exhibited the capabilities of *A. niger* to grow weakly on a plate containing 1% ethanol as a sole carbon source (O'Connell & Kelly, 1988). However, while *A. niger* was demonstrated to be capable of tolerating some concentrations of ethanol in many cases, and while a transcriptomic analysis of its closely related fungus *Aspergillus nidulans* revealed a 10-fold and twofold upregulation of alcohol dehydrogenase *alcA* and *aldA* genes in minimal medium containing ethanol compared with glucose, respectively (Mogensen, Nielsen, Hofmann, & Nielsen, 2006), there have so far been no reports on the metabolic responses of *A. niger* toward ethanol. The knowledge of which would allow for the engineering of the strain to have either higher tolerance toward ethanol for utilization in biotechnological industry or for designing novel methods for eradication of the strain in unwanted situations, such as in food spoilage or on a wall of an ethanol tank. We therefore decided to study the metabolic responses of *A. niger* ES4 toward ethanol further.

In this study, ethanol tolerance of *A. niger* ES4 was first examined. Then, to understand its metabolic responses toward ethanol, untargeted metabolomics analysis was conducted to assay extracellular and intracellular hydrophobic compound changes in *A. niger* ES4 when put under ethanol stress. Lastly, since it was possible that this strain of *A. niger* might intake ethanol for nutrients or substrates for production of some metabolites, the incorporation of ethanol into its metabolites was interrogated by stable isotope labeling mass spectrometry (MS) experiments using ethanol-d_6.

2 | MATERIALS AND METHODS

2.1 | Fungal strain and growth conditions

Aspergillus niger strain ES4 was isolated from a black spot on the outside upper wall of an ethanol tank of a petroleum company by the serial dilution method (Clark, Bordner, Galdrich, Kabler, & Huff, 1958). It was identified based on morphological characteristics and then confirmed using molecular technique. The nucleotide sequence data were submitted into the DDBJ/EMBL/GenBank nucleotide sequence databases with accession number MK621333.

The fungus was grown on potato dextrose agar for 7 days, before three agar plugs were inoculated in 20 ml of potato dextrose broth and shaken at 180 rpm, room temperature for 3 days. The culture was then diluted 20-fold into 20 ml of minimal medium (MM; per liter: 6 g $NaNO_3$, 0.52 g KCl, 0.52 g $MgSO_4.7H_2O$, 1.52 g KH_2PO_4, 10 g glucose, 2 ml Hutner's trace elements, pH 6.8) (Barratt, Johnson, & Ogata, 1965) with ethanol (Merck, absolute, ≥99.9%), water (as control), or ethanol-d_6 (Merck, deuteration degree ≥ 99%; for stable isotope labeling MS) at the indicated concentrations and shaken further until the predetermined time.

2.2 | Determination of the dry weight

Mycelia from three 20-ml cultures were combined and collected on a dry, preweighed Whatman paper no. 1 by vacuum filtration. They were then washed with distilled water (4 × 5 ml, then 2 × 20 ml) and dried on the filter paper at 70°C until at a constant weight (dry weight [DW]).

2.3 | Metabolites extraction and analysis

Mycelia and supernatant from the 3-day-old 20-ml *A. niger* culture were separated by gravity filtration through a cotton ball. A mixture of 10 ml of chloroform and 5 ml of methanol was added to the supernatant, while mycelia were washed once with 10 ml of distilled water and soaked overnight in a mixture of 3 ml of chloroform and 1.5 ml of methanol, before 1.5 ml of MM without glucose was added to them. Subsequently, all mixtures were shaken vigorously, and centrifuged

at 1500 *g*, room temperature for 3 min to separate the organic layer (bottom) from the aqueous layer (top). The organic layer was transferred to another glass vial, evaporated to dryness under a steam of nitrogen, and placed at −20°C for storage. The extracts were reconstituted in 200 µl of chloroform prior to analysis by liquid chromatography (LC)–MS.

For LC–MS and LC–MS/MS analyses, 40 µl of each sample was quantitated on an Ultimate DGP-3600SD LC coupled to a Bruker MicrOTOF Q-II MS instrument, both in the positive and negative ion modes, as described previously (Vinayavekhin et al., 2016).

2.4 | LC–MS untargeted data analysis

The total ion chromatograms from each sample group (i.e., control vs. ethanol treatment) were obtained in triplicate. The total of six chromatograms for mycelia samples and six chromatograms for supernatant samples were then subjected to comparative data analyses separately as previously described (Vinayavekhin, Mahipant, Vangnai, & Sangvanich, 2015), except that (a) the data were normalized by the average DW of the cultures instead of the optical density at 600 nm and (b) the minimum integrated mass ion intensity (MSII) was set at 5,000 instead of 30,000.

2.5 | Stable isotope labeling MS with ethanol-d_6

Intracellular metabolites from *A. niger* cultures treated with ethanol-d_6 were extracted and analyzed by LC–MS exactly as described above in the section "2.3 Metabolites extraction and analysis." The resulting chromatograms were then inspected manually to obtain the mass spectra of the indicated ions.

3 | RESULTS

3.1 | Ethanol tolerance of *A. niger* ES4

Since *A. niger* ES4 was isolated from the outside upper wall of an ethanol tank, we first assessed its ethanol tolerance. It, however, was not possible to monitor the growth of *A. niger* on the solid agar medium containing ethanol, which best mimicked its growth on the wall of the tank, because its spore interfered with the radial growth (data not shown). We therefore determined its ethanol tolerance using a cell growth assay in a defined liquid medium instead (Mahipant et al., 2017). In this assay, *A. niger* ES4 mycelia (60 ml) were cultured in MM adapted slightly from that used by Barratt et al. (1965) for culturing *Aspergillus nidulans*, and with ethanol added at concentrations up to 5% (*v*/*v*). Then, their growth was monitored daily over a 5-day period by measuring the DW of mycelia.

The *A. niger* strain ES4 was able to grow in ethanol at all tested concentrations (2%–5% [*v*/*v*]), although at slower growth rates than the no-ethanol control (Figure 1). Increasing ethanol concentrations decreased the DW at each measured time point in a dose-dependent manner and became lowest at 5% (*v*/*v*) ethanol. The DW amounted to 78%, 65%, 49%, and 30% of that of the ethanol-free control at 2%, 3%, 4%, and 5% (*v*/*v*) ethanol, respectively, at day 4 when the cells were solidly in the stationary phase. Overall, the data revealed some degree of tolerance toward ethanol by the *A. niger* ES4 strain.

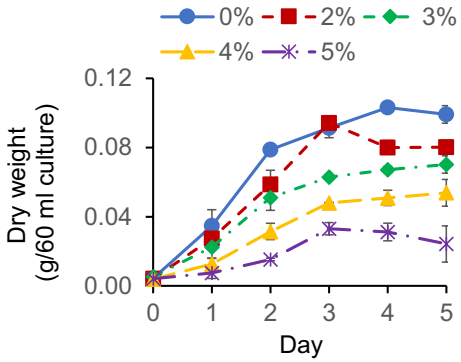

FIGURE 1 Growth curves of *A. niger* ES4 in MM with concentrations of ethanol from 0% to 5% (*v*/*v*). Data are shown as the average DW of mycelia from a 60-ml culture ± standard error of the mean for triplicate experiments per concentration

3.2 | Metabolomics of *A. niger* under ethanol stress

To further characterize the microbe and understand the responses of *A. niger* toward ethanol, metabolomics analysis was performed on both the extracellular and intracellular components of *A. niger* ES4 cultures in the presence and absence of 4% (*v*/*v*) ethanol at day 3, which was the condition that induced moderate stress levels to the fungi (i.e., 52% growth of that without ethanol) and at the day the cells entered early stationary phase (Figure 1). The mycelia or culture supernatant was then extracted for analysis of the hydrophobic metabolites using a 2:1 (*v*/*v*) ratio of chloroform:methanol, and the extracts were concentrated and analyzed by LC–MS using a previously developed untargeted metabolomics platform (Vinayavekhin et al., 2015).

To identify differential metabolites related to ethanol stress responses, the XCMS program (Smith, Want, O'Maille, Abagyan, & Siuzdak, 2006) was used to obtain an MSII value for each detectable metabolite ion in each LC–MS chromatogram, and the MSII values were normalized by the DW to account for the differences in fungal growth. Ions were then regarded as potential responses to ethanol stress only if they were up- or downregulated by fourfold or more with statistical significance (Student's *t* test with $p < .05$) in the ethanol-treated samples compared with the controls, and only if they also met these criteria in another set of independent experimental repeat. Using these criteria, the unbiased comparative analyses revealed 68 and 7 upregulated ions and 1 and 1 downregulated ions in the supernatant, and 322 and 29 upregulated ions and 14 and 24 downregulated ions in the mycelia under ethanol stress in the positive and negative ion modes, respectively (Figure 2).

Next, the structural characterization of these ions with altered levels following ethanol treatment was undertaken manually using the combined clues from the accurate mass, previously reported retention time (RT) (Vinayavekhin et al., 2015, 2016), and tandem mass

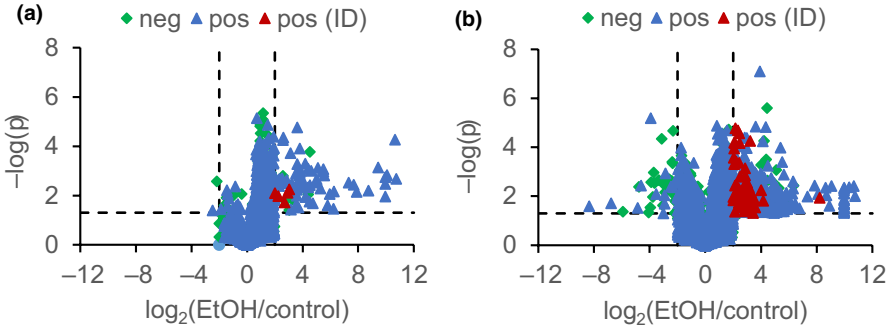

FIGURE 2 Volcano plots of metabolite changes in *A. niger* ES4 at day 3 caused by 4% (*v*/*v*) ethanol. Each (a) extracellular and (b) intracellular metabolite ion in the hydrophobic components with an average MSII above 5,000 counts is plotted as its statistical significance (*p*-value) against the fold change of ethanol (EtOH) over the control. The ions that locate above the horizontal dash line and outside the two vertical dash lines have a *p*-value of less than 0.05 and a fold change of greater than 4, respectively. Each plot contains data from both negative (neg) and positive (pos) ion modes. However, only some positive-mode MS ions with $p < .05$ could be identified (pos (ID)) in this study

spectra (Appendix 1: Tables A1 and A2, and Figure S1). Structures could be assigned to five extracellular and 63 intracellular upregulated positive-mode ions. All of these ions were in the family of triacylglycerol (TAG) for the extracellular components, and the families of diacylglycerol (DAG), TAG, and hydroxy-(h)TAG for the intracellular components (Table 1, and Appendix 1: Tables A1 and A2 with the *sn*-1, *sn*-2 and *sn*-3 side chains written in random order and exact positions of the hydroxyl groups on hTAG unspecified). The most commonly found acyl chains in these altered lipids were 16:0, 18:0, 18:1, and 18:2. The remaining uncharacterized changed ions could not be grouped into the same families as other changed ions, were detected at relatively lower MSII, or were potentially classified as ion fragments or adducts of other smaller or larger molecules. As references, we also performed targeted analyses of other lipids in the biosynthetic pathways of DAG and TAG, such as phospholipids (see Figure 3 for details), and found their levels under ethanol stress more or less undifferentiated from those of the controls (Table 1, Appendix 1: Table A3, and Figure S1). Together, the untargeted metabolomics analysis suggested the involvement of glycerolipids in response to ethanol stress in *A. niger* ES4.

3.3 | Ethanol utilization by *A. niger* ES4

To survive on the wall of an ethanol tank, it might be necessary for *A. niger* strain ES4 to be capable of metabolizing ethanol for nutrients or incorporating ethanol into other molecules to reduce its toxicity. Because our metabolomics analyses above revealed the upregulation of DAG, TAG, and hTAG in the ethanol-treated *A. niger* samples compared with the controls, we set out to trace the possible incorporation of ethanol or parts of ethanol into some of these lipids by using stable isotope labeling MS with ethanol-d_6.

The *A. niger* ES4 cultures were grown in MM in the presence of 4% (*v*/*v*) ethanol-d_6 (or nonlabeled ethanol as controls) for 3 days, harvested for metabolites in the mycelia, and analyzed by LC–MS exactly as described earlier for metabolomics. The chromatograms were then inspected manually for the mass spectra of four representative metabolite ions: (a) DAG (18:2/18:2), (b) TAG (18:0/18:1/18:1) (significantly elevated under ethanol treatment compared to the untreated controls), (c) fatty acid (FA) (18:2), and (d) phosphatidic acid (PA) (18:2/18:2) (in the related metabolic pathways but with unchanged levels). The data showed varying shift in the detected mass-to-charge ratios (m/z) of all lipids in the ethanol-d_6 samples from the nonlabeled controls (Figure 4). The monoisotopic peaks of all lipids, except for FA (18:2), in the nonlabeled samples were no longer dominant peaks in the ethanol-d_6 samples. The m/z with the highest intensities were shifted by +3, +5, and +2 mass units for DAG (18:2/18:2), TAG (18:0/18:1/18:1), and PA (18:2/18:2) from those in the nonlabeled samples, respectively. However, the m/z peaks at ±1, ±2, and ±3 mass units from the dominant m/z peaks were not very different in intensities from those of the dominant m/z peaks for all investigated lipids in the ethanol-d_6 samples. Overall, the results support the metabolism of ethanol in *A. niger* ES4 into other metabolites.

4 | DISCUSSION

The ability to tolerate chemicals present in cultures is one of the most essential traits of microorganisms for utilization in bioprocesses. In this study, we found *A. niger* ES4 capable of growing even in 5% (*v*/*v*) (or 4% [*w*/*v*]) ethanol with its growth amounting to approximately 30% of that of the ethanol-free control. Interestingly, this level of tolerance was comparable with that of the ethalogenic filamentous fungus *Fusarium oxysporum* (Paschos, Xiros, & Christakopoulos, 2015) and higher than that of the natural ethanol-producing ascomycetous yeasts *Pichia stipites*, whose growth was inhibited at 3.4% (*w*/*v*) ethanol when grown on glucose (Meyrial, Delgenes, Romieu, Moletta, & Gounot, 1995). Assuming that the amount of ethanol produced by these ethalogenic microbes themselves stayed relatively low compared with that of the initially added ethanol concentration, our results would indicate that *A. niger* strain ES4 had a relatively high resistance toward ethanol. However, as mentioned earlier, Dantigny et al. (2005) also demonstrated the ability of the *A. niger*

TABLE 1 Relative levels of identified ethanol-upregulated lipids and of other related lipids

Lipid class and acyl chain	Ion	m/z	RT (min)	EtOH/con[a,b]
Upregulated lipids in ethanol-treated extracellular samples				
Triacylglycerol (TAG)				
16:0/18:1/18:2	$[M + NH_4]^+$	874.7830	48.3	4.8*
18:1/18:2/18:2	$[M + NH_4]^+$	898.7839	48.1	6.6*
18:1/18:1/18:2	$[M + NH_4]^+$	900.7989	48.6	4.1†
18:1/18:1/18:1	$[M + NH_4]^+$	902.8136	48.7	7.7†
18:0/18:1/18:1	$[M + NH_4]^+$	904.8272	48.9	8.3†
Upregulated lipids in ethanol-treated intracellular samples				
Diacylglycerol (DAG)				
18:2/18:2	$[M + NH_4]^+$	634.5394	43.8	7.5*
18:1/18:2	$[M + NH_4]^+$	636.5550	44.4	6.7*
18:1/18:1	$[M + NH_4]^+$	638.5700	44.9	6.7†
18:0/18:1	$[M + NH_4]^+$	640.5815	45.3	8.7†
18:2/20:2	$[M + NH_4]^+$	662.5667	44.6	8.0*
18:2/20:1	$[M + NH_4]^+$	664.5833	45.1	7.0*
TAG				
12:0/18:2/18:2	$[M + NH_4]^+$	816.7036	47.6	8.4†
14:0/18:2/18:2	$[M + NH_4]^+$	844.7360	47.8	4.4‡
18:0/18:1/18:1	$[M + NH_4]^+$	904.8319	49.0	4.5§
18:0/18:0/18:1	$[M + NH_4]^+$	906.8451	49.1	5.4§
18:0/18:1/20:0	$[M + NH_4]^+$	934.8749	49.5	4.4§
18:0/18:1/24:0	$[M + NH_4]^+$	990.9377	50.2	4.1§
18:1/18:1/25:0	$[M + NH_4]^+$	1,002.9375	50.2	5.0†
18:0/18:1/26:0	$[M + NH_4]^+$	1,018.9654	50.5	4.7§
Hydroxy-TAG (hTAG)				
16:0/16:1(OH)/18:2	$[M + NH_4]^+$	862.7455	46.9	4.6‡
16:0/16:0/18:2(OH)	$[M + NH_4]^+$	864.7565	47.2	4.2§
16:0/18:2/18:2(OH)	$[M + NH_4]^+$	888.7606	47.1	8.2*
16:0/18:1/18:2(OH)	$[M + NH_4]^+$	890.7736	47.3	5.4†
18:1/18:2(OH)/18:3	$[M + NH_4]^+$	912.7626	46.9	11.2*
18:1/18:2/18:2(OH)	$[M + NH_4]^+$	914.7771	47.2	11.8*
18:1/18:1/18:2(OH)	$[M + NH_4]^+$	916.7929	47.5	8.8‡
18:0/18:1/18:2(OH)	$[M + NH_4]^+$	918.8068	47.7	9.9†
Other intracellular lipids in the related pathways				
Fatty acid (FA)				
16:0	$[M - H]^-$	255.2317	18.6	1.6†
18:2	$[M - H]^-$	279.2336	18.5	1.7†
18:1	$[M - H]^-$	281.2478	18.8	2.0‡
18:0	$[M - H]^-$	283.2624	19.2	1.5‡
Monoacylglycerol (MAG)				
16:0	$[M + Na]^+$	353.2656	34.0	2.4*
18:2	$[M + Na]^+$	377.2718	33.1	2.1
Phosphatidic acid (PA)				
16:0/18:2	$[M-H]^-$	671.4649	27.4	1.6
18:2/18:2	$[M-H]^-$	695.4647	26.8	2.3*

(Continues)

TABLE 1 (Continued)

Lipid class and acyl chain	Ion	m/z	RT (min)	EtOH/con[a,b]
Phosphatidylethanolamine (PE)				
16:0/18:2	$[M - H]^-$	714.5023	39.0	1.0
18:2/18:2	$[M - H]^-$	738.5004	38.2	1.7
Phosphatidylserine (PS)				
16:0/18:2	$[M - H]^-$	758.4944	29.9	1.3
18:2/18:2	$[M - H]^-$	782.4946	29.3	1.5
Phosphatidylglycerol (PG)				
16:0/18:2	$[M - H]^-$	745.4976	34.4	1.4
18:2/18:2	$[M - H]^-$	769.4962	33.8	1.5
Phosphatidylinositol (PI)				
16:0/18:2	$[M - H]^-$	833.5160	34.0	1.2
18:2/18:2	$[M - H]^-$	857.5147	33.4	1.1
Phosphatidylcholine (PC)				
16:0/18:2	$[M + H]^+$	758.5726	41.7	0.8†
18:2/18:2	$[M + H]^+$	782.5751	41.3	1.8§

Abbreviations: m/z, mass-to-charge ratio; RT, retention time.
[a]EtOH/con value represents the ratio of the average mass ion intensity of ethanol-treated sample group and that of the control.
[b]Student's *t* test: *, $p < .05$; †, $p < .01$; ‡, $p < .005$; §, $p < .001$; $N = 3$.

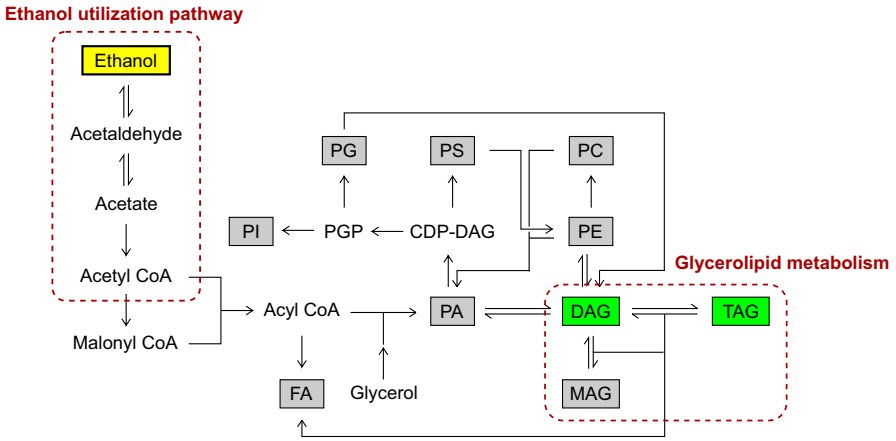

FIGURE 3 Biosynthesis of glycerolipids and phospholipids in *A. niger* (Kanehisa & Goto, 2000), starting from ethanol. The *green boxes* indicate lipids that had statistically significantly elevated levels, whereas the *gray boxes* show other lipids whose levels were quantitated in this study and the *yellow box* emphasizes where ethanol locates in the pathways. Glycerolipids include monoacylglycerol (MAG), diacylglycerol (DAG), and triacylglycerol (TAG), whereas phospholipids shown are phosphatidic acid (PA), phosphatidylethanolamine (PE), phosphatidylcholine (PC), phosphatidylserine (PS), phosphatidylglycerol (PG), and phosphatidylinositol (PI)

strain isolated from spoiled pastry products to grow on potato dextrose agar containing ethanol up to 4% (*w*/*w*) with about 50% reduction in its growth, which seemed to be higher than ethanol tolerance of *A. niger* ES4 in this study. Nevertheless, it was known that the choice of culture media and conditions could affect ethanol tolerance of microbes greatly, and thus, how tolerance *A. niger* ES4 is compared to other *A. niger* strains or other organisms remained to be proven in the future study.

The subsequent investigation into the response mechanisms of *A. niger* ES4 to ethanol using an untargeted metabolomics approach revealed the accumulation of neutral glycerolipids (extracellular TAG, and intracellular DAG, TAG, and hTAG) under ethanol stress. DAG and TAG are interconnected in the glycerolipid metabolism (Figure 4). Functionally, DAG is known to play multiple roles from being a component of the cell membrane and an intermediate in lipid metabolism to a second messenger in lipid-mediated signaling cascades (Carrasco & Mérida, 2007), whereas TAG is traditionally thought of as an energy storage lipid.

In terms of responses to stress, even though there have been no prior reports demonstrating the effect of upregulated DAG or TAG in the organic solvent tolerance of microbes, these neutral lipids were previously implicated in protecting plants from other abiotic

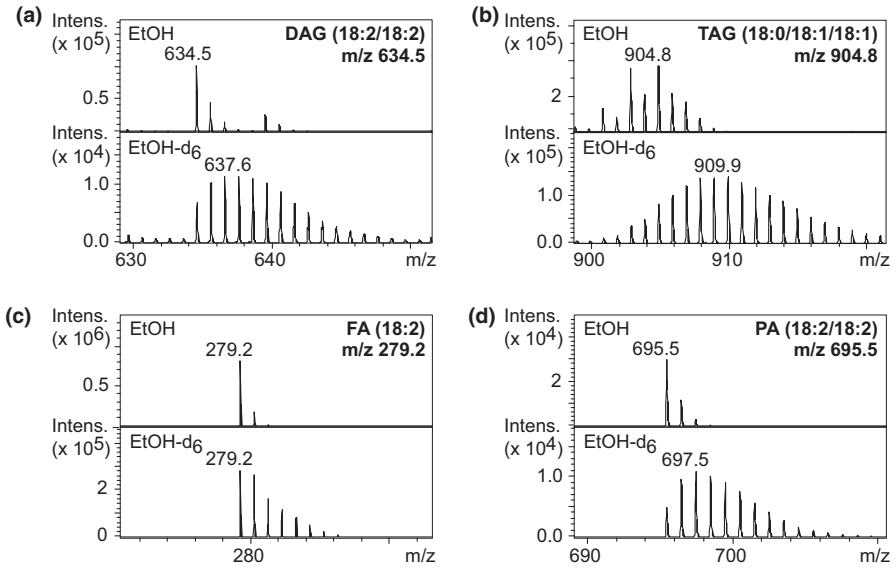

FIGURE 4 Mass spectra of representative ions from stable isotope labeling MS experiments with ethanol-d_6. The *A. niger* ES4 was cultured in duplicate in the presence of 4% (v/v) either ethanol (EtOH)-d_6 or EtOH (as control) and analyzed for intracellular metabolites exactly as conducted in the untargeted metabolomics analysis. Mass spectra were extracted from the total ion chromatograms at the retention time (RT) of 43.8 min for (a) diacylglycerol (DAG) (18:2/18:2) and 49.0 min for (b) triacylglycerol (TAG) (18:0/18:1/18:1) in the positive ion mode, and at a RT of 18.5 min for (c) fatty acid (FA) (18:2) and 26.8 min for (d) phosphatidic acid (PA) (18:2/18:2) in the negative ion mode

stressors, such as coldness (Tan et al., 2018) and darkness (Fan, Yu, & Xu, 2017). In the case of coldness, for example, *Arabidopsis* accumulated PA, DAG, and TAG during freezing stress where disruption in the genes encoding the enzymes acyl-coenzyme A: DAG acyltransferase and DAG kinase, which catalyze the conversion of DAG to TAG and PA, subsequently resulted in decreased and increased TAG levels and tolerance to coldness, respectively (Tan et al., 2018). It is, therefore, possible that, with the unchanged levels of other phospholipids that are components of cell membranes (e.g., PA, phosphatidylethanolamine (PE), and phosphatidylcholine (PC) [Ianutsevich, Danilova, Groza, & Tereshina, 2016]) found in this study, the elevated DAG and TAG levels as the novel responses to ethanol stress might play some roles in defending *A. niger* against the toxic effects of ethanol. Yet, because cold stress rigidifies cell membrane, the effect that is opposite to that of ethanol, further genetic data are needed to pinpoint the relevance of these glycerolipids on ethanol tolerance of *A. niger*. In addition, it remains to be determined whether the upregulation in glycerolipids following ethanol exposure is specific to *A. niger* ES4 or general for all *A. niger* isolates.

Another class of metabolites elevated under ethanol stress was hTAGs, which have mainly been described in *Ricinus communis* castor oil (Kim et al., 2011), *Lesquerella* seed oil (Byrdwell & Neff, 1998; Hayes, Kleiman, & Phillips, 1995), and ergot oil from the fungus *Claviceps purpurea* (Morris & Hall, 1966). As the detection and quantitation of hTAG in routine work have remained quite limited compared with other classes of lipids, there is no evidence to support or refute their relevance to various stresses. Yet, because their substrates, hydroxy fatty acids, are known for their specialized medical and industrial usages (e.g. lubricants, paints, and coatings) (Hayes et al., 1995; Meesapyodsuk & Qiu, 2008), the discovery of upregulated hTAGs in this study suggested that, upon fully characterizing their structures, *A. niger* might be able to serve as another source of this industrially important class of lipids as well.

One of the known metabolic responses of the yeast *Saccharomyces cerevisiae* toward ethanol involves an increase in the unsaturated-to-saturated fatty acids ratio, whereby the relative contents of FA (16:1) and FA (18:1) increase while those of FA (16:0) and FA (18:0) decrease (Sajbidor, Ciesarova, & Smogrovicova, 1995). Interestingly, our metabolomics studies showed only slight elevation in contents of all four most abundant fatty acids found in *A. niger* ES4 (i.e., 16:0, 18:2, 18:1 and 18:0) under ethanol stress without an obvious shift in unsaturation index. The alteration in this index was also not immediately apparent in other lipid species, as most of the changing lipids contained both unsaturated and saturated acyl chains. The findings therefore suggested that *A. niger* might utilize different mechanisms to counteract toxicity of ethanol than *S. cerevisiae*. However, we could not rule out the possibilities that the observed effects might simply be specific to the choices of microbial strain, growth medium, or conditions depicted in this study.

The results from the stable isotope labeling MS showed that the isotopic patterns of all the molecular ions of representative lipids in the ethanol-d_6 samples differed from those in the nonlabeled ethanol samples. Because the only isotope present at an unnaturally high abundance in this case was deuterium, the finding indicated the incorporation of varying numbers of deuterium atoms into each lipid, which could potentially occur both via catabolism of ethanol-d_6 by *A. niger* and via deuterium exchanges with the deuteron on the hydroxyl group of ethanol-d_6 during the lipid biosynthesis.

However, in this study, ethanol-d_6 was added into the cultures at 4% (*v*/*v*), which resulted in the mole ratio of proton to deuteron in the cultures being 100 to 0.58 (see Appendix 2 for details on calculation). Assuming that all hydrogen atoms on each representative ion have equal chances to undergo deuterium exchanges, and disregarding any kinetics isotope effects of deuterium, the predicted isotopic ratios, M:M + 1:M + 2:M + 3:M + 4, when considering only deuterium exchanges and natural isotopic abundance of each element would be equal to 100:84:36:10:2 for DAG (18:2/18:2), 80:100:63:27:9 for TAG (18:0/18:1/18:1), 100:38:7:1:<1 for FA (18:2), and 100:82:35:10:2 for PA (18:2/18:2) (Appendix 2). These ratios represent the highest probable signals of each isotope arisen from deuterium exchanges; yet, they alone still could not account for the observed high abundances of these isotopes, especially with M + 2 and higher m/z species, in the ethanol-d_6 samples (Figure 3). The finding therefore suggested to us that *A. niger* ES4 was in fact capable of metabolizing ethanol-d_6 into other compounds in an existing metabolic pathway.

Metabolically, the ethanol utilization pathway has been well studied in the closely related fungus, *Aspergillus nidulans* (Felenbok, Flipphi, & Nikolaev, 2001). In this pathway, ethanol is first oxidized to acetaldehyde by alcohol dehydrogenase I. Further oxidation of acetaldehyde by alcohol dehydrogenase then yields acetate, which subsequently is converted to acetyl CoA by acetyl CoA synthetase (Figure 3). In the form of acetyl CoA, these carbon and hydrogen atoms from ethanol can then enter into many metabolic pathways, along with the acetyl CoA synthesized from other carbon sources, such as glucose. For lipid synthesis, acetyl CoA is carboxylated to malonyl CoA and coupled with this product to yield acyl CoA, which is the substrate for production of fatty acids, phospholipids, and glycerolipids (Figure 3) (Kanehisa & Goto, 2000). For *A. niger*, the genes encoding several homologs of alcohol dehydrogenases have been annotated in the genome of *A. niger* strain CBS513.88 (Pel et al., 2007). However, their activities in culture have not been confirmed. Our present data, therefore, represent the first piece of evidence to support the existence of this ethanol utilization pathway in *A. niger* ES4.

5 | CONCLUSIONS

In total, by applying untargeted metabolomics to study the extracellular and intracellular hydrophobic components of the *A. niger* strain ES4 isolated from the wall of an ethanol tank, we demonstrated the upregulation of glycerolipids (i.e., DAG, TAG and hTAG) as novel responses of microbes to ethanol stress. The subsequent stable isotope labeling MS with ethanol-d_6 also supported the utilization of ethanol by *A. niger* ES4. Future work will aim to determine the relevance of these upregulated changes in glycerolipid metabolism and the ethanol utilization pathway in the ethanol tolerance of *A. niger*, as well as to elucidate the structures, biosynthesis, and functions of hTAG more thoroughly. More generally, we believe that untargeted metabolomics platforms and the overall approaches presented in this work will be powerful tools for the discovery of more novel responses of microbes to organic solvent stress, as well as to other external stimuli, in the future.

ACKNOWLEDGEMENTS

We thank Dr. Robert Douglas John Butcher (Research Clinic Unit, Office of Research Affairs, Chulalongkorn University) for editorial help in preparing this manuscript. This research was supported by the Office of the Higher Education Commission and the Thailand Research Fund (MRG6180002). The opinions expressed in this paper are the sole responsibility of the authors and do not necessarily reflect those of the funding agencies or Chulalongkorn University.

CONFLICT OF INTEREST

None declared.

AUTHOR CONTRIBUTIONS

Nawaporn Vinayavekhin coordinated the experiments, analyzed the data, drafted, and revised the manuscript. Wimonsiri Kongchai conducted the experiments and analyzed the data. Jittra Piapukiew and Warinthorn Chavasiri discussed the experiments and revised the manuscript. All authors read and approved the final version of the manuscript.

ETHICAL APPROVAL

None required.

DATA AVAILABILITY STATEMENT

The nucleotide sequence data were deposited into the DDBJ/EMBL/GenBank nucleotide sequence databases with accession number MK621333. Other data generated or analyzed during this study are included in this published article and its Supporting Information file.

ORCID

Nawaporn Vinayavekhin https://orcid.org/0000-0002-1525-0382

Jittra Piapukiew https://orcid.org/0000-0003-0116-590X

Warinthorn Chavasiri https://orcid.org/0000-0001-5201-1324

REFERENCES

Aono, R., & Kobayashi, H. (1997). Cell surface properties of organic solvent-tolerant mutants of *Escherichia coli* K-12. *Applied and Environmental Microbiology*, *63*(9), 3637–3642.

Aono, R., Tsukagoshi, N., & Yamamoto, M. (1998). Involvement of outer membrane protein TolC, a possible member of the mar-sox regulon,

in maintenance and improvement of organic solvent tolerance of *Escherichia coli* K-12. *Journal of Bacteriology*, *180*(4), 938–944.

Baker, S. E. (2006). *Aspergillus niger* genomics: Past, present and into the future. *Medical Mycology*, *44*, S17–S21. https://doi.org/10.1080/13693780600921037

Barratt, R. W., Johnson, G. B., & Ogata, W. N. (1965). Wild-type and mutant stocks of *Aspergillus nidulans*. *Genetics*, *52*(1), 233–246.

Bohin, J. P., Rigomier, D., & Schaeffer, P. (1976). Ethanol sensitivity of sporulation in *Bacillus subtilis*: A new tool for the analysis of the sporulation process. *Journal of Bacteriology*, *127*(2), 934–940.

Bustard, M. T., Whiting, S., Cowan, D. A., & Wright, P. C. (2002). Biodegradation of high-concentration isopropanol by a solvent-tolerant thermophile. *Bacillus Pallidus*. *Extremophiles*, *6*(4), 319–323. https://doi.org/10.1007/s00792-001-0260-5

Byrdwell, W. C., & Neff, W. E. (1998). Analysis of hydroxy-containing seed oils using atmospheric pressure chemical ionization mass spectrometry. *Journal of Liquid Chromatography & Related Technologies*, *21*(10), 1485–1501. https://doi.org/10.1080/10826079808000529

Carrasco, S., & Mérida, I. (2007). Diacylglycerol, when simplicity becomes complex. *Trends in Biochemical Sciences*, *32*(1), 27–36. https://doi.org/10.1016/j.tibs.2006.11.004

Clark, D. S., Bordner, P., Galdrich, E. H., Kabler, P. W., & Huff, C. B. (1958). *Applied Microbiology*. New York, NY: International Book Company.

Coulibaly, L., Naveau, H., & Agathos, S. N. (2002). A tanks-in-series bioreactor to simulate macromolecule-laden wastewater pretreatment under sewer conditions by *Aspergillus niger*. *Water Research*, *36*(16), 3941–3948. https://doi.org/10.1016/S0043-1354(02)00117-3

Dantigny, P., Guilmart, A., Radoi, F., Bensoussan, M., & Zwietering, M. (2005). Modelling the effect of ethanol on growth rate of food spoilage moulds. *International Journal of Food Microbiology*, *98*(3), 261–269. https://doi.org/10.1016/j.ijfoodmicro.2004.07.008

Fan, J., Yu, L., & Xu, C. (2017). A central role for triacylglycerol in membrane lipid breakdown, fatty acid beta-oxidation, and plant survival under extended darkness. *Plant Physiology*, *174*(3), 1517–1530. https://doi.org/10.1104/pp.17.00653

Felenbok, B., Flipphi, M., & Nikolaev, I. (2001). Ethanol catabolism in *Aspergillus nidulans*: A model system for studying gene regulation. *Progress in Nucleic Acid Research and Molecular Biology*, *69*, 149–204. https://doi.org/10.1016/S0079-6603(01)69047-0

Frisvad, J. C., Larsen, T. O., Thrane, U., Meijer, M., Varga, J., Samson, R. A., & Nielsen, K. F. (2011). Fumonisin and ochratoxin production in industrial *Aspergillus niger* strains. *PLoS ONE*, *6*(8), e23496. https://doi.org/10.1371/journal.pone.0023496

Hayes, D. G., Kleiman, R., & Phillips, B. S. (1995). The triglyceride composition, structure, and presence of estolides in the oils of *Lesquerella* and related species. *Journal of the American Oil Chemists Society*, *72*(5), 559–569. https://doi.org/10.1007/Bf02638857

Ianutsevich, E. A., Danilova, O. A., Groza, N. V., & Tereshina, V. M. (2016). Membrane lipids and cytosol carbohydrates in *Aspergillus niger* under osmotic, oxidative, and cold impact. *Microbiology*, *85*(3), 302–310. https://doi.org/10.1134/S0026261716030152

Izmirlioglu, G., & Demirci, A. (2017). Simultaneous saccharification and fermentation of ethanol from potato waste by co-cultures of *Aspergillus niger* and *Saccharomyces cerevisiae* in biofilm reactors. *Fuel*, *202*, 260–270. https://doi.org/10.1016/j.fuel.2017.04.047

Kajiwara, S., Shirai, A., Fujii, T., Toguri, T., Nakamura, K., & Ohtaguchi, K. (1996). Polyunsaturated fatty acid biosynthesis in *Saccharomyces cerevisiae*: Expression of ethanol tolerance and the FAD2 gene from *Arabidopsis thaliana*. *Applied and Environmental Microbiology*, *62*(12), 4309–4313.

Kanehisa, M., & Goto, S. (2000). KEGG: Kyoto encyclopedia of genes and genomes. *Nucleic Acids Research*, *28*(1), 27–30. https://doi.org/10.1093/nar/28.1.27

Kang, H.-J., Heo, D.-H., Choi, S.-W., Kim, K.-N., Shim, J., Kim, C.-W., … Yun, C.-W. (2007). Functional characterization of Hsp33 protein from *Bacillus psychrosaccharolyticus*; additional function of HSP33 on resistance to solvent stress. *Biochemical and Biophysical Research Communications*, *358*(3), 743–750. https://doi.org/10.1016/j.bbrc.2007.04.184

Kim, H. U., Lee, K. R., Go, Y. S., Jung, J. H., Suh, M. C., & Kim, J. B. (2011). Endoplasmic reticulum-located PDAT1-2 from castor bean enhances hydroxy fatty acid accumulation in transgenic plants. *Plant and Cell Physiology*, *52*(6), 983–993. https://doi.org/10.1093/pcp/pcr051

Lubertozzi, D., & Keasling, J. D. (2009). Developing *Aspergillus* as a host for heterologous expression. *Biotechnology Advances*, *27*(1), 53–75. https://doi.org/10.1016/j.biotechadv.2008.09.001

Mahipant, G., Paemanee, A., Roytrakul, S., Kato, J., & Vangnai, A. S. (2017). The significance of proline and glutamate on butanol chaotropic stress in *Bacillus subtilis* 168. *Biotechnology for Biofuels*, *10*, 122. https://doi.org/10.1186/s13068-017-0811-3

Meesapyodsuk, D., & Qiu, X. (2008). An oleate hydroxylase from the fungus *Claviceps purpurea*: Cloning, functional analysis, and expression in *Arabidopsis*. *Plant Physiology*, *147*(3), 1325–1333. https://doi.org/10.1104/pp.108.117168

Meyrial, V., Delgenes, J. P., Romieu, C., Moletta, R., & Gounot, A. M. (1995). Ethanol tolerance and activity of plasma-membrane ATPase in *Pichia stipitis* grown on D-xylose or on D-glucose. *Enzyme and Microbial Technology*, *17*(6), 535–540. https://doi.org/10.1016/0141-0229(94)00065-Y

Mogensen, J., Nielsen, H. B., Hofmann, G., & Nielsen, J. (2006). Transcription analysis using high-density micro-arrays of *Aspergillus nidulans* wild-type and *creA* mutant during growth on glucose or ethanol. *Fungal Genetics and Biology*, *43*(8), 593–603. https://doi.org/10.1016/j.fgb.2006.03.003

Morris, L. J., & Hall, S. W. (1966). The structure of the glycerides of ergot oils. *Lipids*, *1*(3), 188–196. https://doi.org/10.1007/BF02531871

Neumann, G., Veeranagouda, Y., Karegoudar, T. B., Sahin, O., Mäusezahl, I., Kabelitz, N., … Heipieper, H. J. (2005). Cells of *Pseudomonas putida* and *Enterobacter* sp. adapt to toxic organic compounds by increasing their size. *Extremophiles*, *9*(2), 163–168. https://doi.org/10.1007/s00792-005-0431-x

Nicolaou, S. A., Gaida, S. M., & Papoutsakis, E. T. (2010). A comparative view of metabolite and substrate stress and tolerance in microbial bioprocessing: From biofuels and chemicals, to biocatalysis and bioremediation. *Metabolic Engineering*, *12*(4), 307–331. https://doi.org/10.1016/j.ymben.2010.03.004

O'Connell, M. J., & Kelly, J. M. (1988). Differences in the regulation of aldehyde dehydrogenase genes in *Aspergillus niger* and *Aspergillus nidulans*. *Current Genetics*, *14*(2), 95–103. https://doi.org/10.1007/BF00569332

Pariza, M. W., & Cook, M. (2010). Determining the safety of enzymes used in animal feed. *Regulatory Toxicology and Pharmacology*, *56*(3), 332–342. https://doi.org/10.1016/j.yrtph.2009.10.005

Paschos, T., Xiros, C., & Christakopoulos, P. (2015). Ethanol effect on metabolic activity of the ethalogenic fungus Fusarium oxysporum. *BMC Biotechnology*, *15*, 15. https://doi.org/10.1186/s12896-015-0130-3

Pel, H. J., de Winde, J. H., Archer, D. B., Dyer, P. S., Hofmann, G., Schaap, P. J., … Stam, H. (2007). Genome sequencing and analysis of the versatile cell factory *Aspergillus niger* CBS 513.88. *Nature Biotechnology*, *25*(2), 221–231. https://doi.org/10.1038/nbt1282

Person, A. K., Chudgar, S. M., Norton, B. L., Tong, B. C., & Stout, J. E. (2010). *Aspergillus niger*: An unusual cause of invasive pulmonary aspergillosis. *Journal of Medical Microbiology*, *59*(Pt 7), 834–838. https://doi.org/10.1099/jmm.0.018309-0

Petersohn, A., Brigulla, M., Haas, S., Hoheisel, J. D., Volker, U., & Hecker, M. (2001). Global analysis of the general stress response of *Bacillus subtilis*. *Journal of Bacteriology*, *183*(19), 5617–5631. https://doi.org/10.1128/JB.183.19.5617-5631.2001

Ramachandran, S., Fontanille, P., Pandey, A., & Larroche, C. (2008). Permeabilization and inhibition of the germination of spores of *Aspergillus niger* for gluconic acid production from glucose. *Bioresource Technology*, *99*(11), 4559–4565. https://doi.org/10.1016/j.biortech.2007.06.055

Sajbidor, J., Ciesarova, Z., & Smogrovicova, D. (1995). Influence of ethanol on the lipid content and fatty acid composition of *Saccharomyces cerevisiae*. *Folia Microbiologica*, *40*(5), 508–510.

Smith, C. A., Want, E. J., O'Maille, G., Abagyan, R., & Siuzdak, G. (2006). XCMS: Processing mass spectrometry data for metabolite profiling using nonlinear peak alignment, matching, and identification. *Analytical Chemistry*, *78*(3), 779–787. https://doi.org/10.1021/ac051437y

Srivastava, S., & Thakur, I. S. (2006). Evaluation of bioremediation and detoxification potentiality of *Aspergillus niger* for removal of hexavalent chromium in soil microcosm. *Soil Biology & Biochemistry*, *38*(7), 1904–1911. https://doi.org/10.1016/j.soilbio.2005.12.016

Tan, W.-J., Yang, Y.-C., Zhou, Y., Huang, L.-P., Xu, L. E., Chen, Q.-F., … Xiao, S. (2018). Diacylglycerol acyltransferase and diacylglycerol kinase modulate triacylglycerol and phosphatidic acid production in the plant response to freezing stress. *Plant Physiology*, *177*(3), 1303–1318. https://doi.org/10.1104/pp.18.00402

Taylor, M., Tuffin, M., Burton, S., Eley, K., & Cowan, D. (2008). Microbial responses to solvent and alcohol stress. *Biotechnology Journal*, *3*(11), 1388–1397. https://doi.org/10.1002/biot.200800158

Torres, S., Pandey, A., & Castro, G. R. (2011). Organic solvent adaptation of Gram positive bacteria: Applications and biotechnological potentials. *Biotechnology Advances*, *29*(4), 442–452. https://doi.org/10.1016/j.biotechadv.2011.04.002

Vinayavekhin, N., Mahipant, G., Vangnai, A. S., & Sangvanich, P. (2015). Untargeted metabolomics analysis revealed changes in the composition of glycerolipids and phospholipids in *Bacillus subtilis* under 1-butanol stress. *Applied Microbiology and Biotechnology*, *99*(14), 5971–5983. https://doi.org/10.1007/s00253-015-6692-0

Vinayavekhin, N., Sueajai, J., Chaihad, N., Panrak, R., Chokchaisiri, R., Sangvanich, P., … Piyachaturawat, P. (2016). Serum lipidomics analysis of ovariectomized rats under *Curcuma comosa* treatment. *Journal of Ethnopharmacology*, *192*, 273–282. https://doi.org/10.1016/j.jep.2016.07.054

Vinayavekhin, N., & Vangnai, A. S. (2018). The effects of disruption in membrane lipid biosynthetic genes on 1-butanol tolerance of *Bacillus subtilis*. *Applied Microbiology and Biotechnology*, *102*(21), 9279–9289. https://doi.org/10.1007/s00253-018-9298-5

Weber, F. J., & de Bont, J. A. (1996). Adaptation mechanisms of microorganisms to the toxic effects of organic solvents on membranes. *Biochimica Et Biophysica Acta (BBA) - Reviews on Biomembranes*, *1286*(3), 225–245. https://doi.org/10.1016/S0304-4157(96)00010-X

SUPPORTING INFORMATION

Additional supporting information may be found online in the Supporting Information section at the end of the article.

How to cite this article: Vinayavekhin N, Kongchai W, Piapukiew J, Chavasiri W. *Aspergillus niger* upregulated glycerolipid metabolism and ethanol utilization pathway under ethanol stress. *MicrobiologyOpen*. 2020;9:e948. https://doi.org/10.1002/mbo3.948

APPENDIX 1

TABLE A1: Identified positive-mode ions with statistically significantly elevated levels in ethanol-treated extracellular *A. niger* samples compared to the untreated control showing the mass-to-charge ratio (*m/z*), retention time (RT) and (a) potential identification and MS/MS spectrum, (b) integrated mass ion intensity (MSII) and (c) adjusted mass ion intensity (aMSII). The MSII and aMSII data are shown for three *A. niger* samples without (Con-1–3) or with ethanol treatment (EtOH-1–3) and their respective averages (Con-avg and EtOH-avg, respectively)

(a) Identified significantly elevated positive-mode ions in ethanol-treated extracellular *A. niger* samples (potential identification and MS/MS spectrum)

No.	*m/z*	RT (min)	Ion	Potential identification	MS/MS spectrum
1	874.7830	48.3	$[M + NH_4]^+$	TAG (16:0/18:1/18:2)	SI, p. S3
2	898.7839	48.1	$[M + NH_4]^+$	TAG (18:1/18:2/18:2)	SI, p. S4
3	900.7989	48.6	$[M + NH_4]^+$	TAG (18:1/18:1/18:2)	SI, p. S5
4	902.8136	48.7	$[M + NH_4]^+$	TAG (18:1/18:1/18:1)	SI, p. S6
5	904.8272	48.9	$[M + NH_4]^+$	TAG (18:0/18:1/18:1)	SI, p. S7

(b) Identified significantly elevated positive-mode ions in ethanol-treated extracellular *A. niger* samples (MSII)

			Integrated mass ion intensity (MSII)							
No.	*m/z*	RT (min)	EtOH-1	EtOH-2	EtOH-3	EtOH-avg	Con-1	Con-2	Con-3	Con-avg
1	874.7830	48.3	3.27E+06	2.51E+06	2.47E+06	2.75E+06	1.30E+06	1.02E+06	9.02E+05	1.07E+06
2	898.7839	48.1	1.01E+07	7.88E+06	6.70E+06	8.24E+06	2.79E+06	2.21E+06	2.08E+06	2.36E+06
3	900.7989	48.6	1.17E+07	8.98E+06	8.84E+06	9.85E+06	8.84E+06	2.66E+06	2.16E+06	4.55E+06
4	902.8136	48.7	7.59E+06	5.94E+06	5.82E+06	6.45E+06	2.02E+06	1.55E+06	1.18E+06	1.58E+06
5	904.8272	48.9	4.85E+06	3.76E+06	4.10E+06	4.23E+06	1.17E+06	9.80E+05	7.42E+05	9.64E+05

(c) Identified significantly elevated positive-mode ions in ethanol-treated extracellular *A. niger* samples (aMSII)

			Adjusted integrated mass ion intensity (aMSII)							
No.	*m/z*	RT (min)	EtOH-1	EtOH-2	EtOH-3	EtOH-avg	Con-1	Con-2	Con-3	Con-avg
1	874.7830	48.3	4.71E+06	3.62E+06	3.55E+06	3.96E+06	9.95E+05	7.83E+05	6.91E+05	8.23E+05
2	898.7839	48.1	1.46E+07	1.13E+07	9.65E+06	1.19E+07	2.14E+06	1.69E+06	1.59E+06	1.81E+06
3	900.7989	48.6	1.69E+07	1.29E+07	1.27E+07	1.42E+07	6.77E+06	2.04E+06	1.65E+06	3.49E+06
4	902.8136	48.7	1.09E+07	8.56E+06	8.38E+06	9.29E+06	1.55E+06	1.19E+06	9.04E+05	1.21E+06
5	904.8272	48.9	6.98E+06	5.41E+06	5.90E+06	6.10E+06	8.95E+05	7.51E+05	5.68E+05	7.38E+05

TABLE A2: Identified positive-mode ions with statistically significantly elevated levels in ethanol-treated intracellular *A. niger* samples compared to the untreated control showing the mass-to-charge ratio (*m/z*), retention time (RT) and (a) potential identification and MS/MS spectrum, (b) integrated mass ion intensity (MSII) and (c) adjusted mass ion intensity (aMSII). The MSII and aMSII data are shown for three *A. niger* samples without (Con-1–3) or with ethanol treatments (EtOH-1–3) and their respective averages (Con-avg and EtOH-avg, respectively)

(a) Identified significantly elevated positive-mode ions in ethanol-treated intracellular *A. niger* samples (potential identification and MS/MS spectrum)

No.	*m/z*	RT (min)	Ion	Potential identification	MS/MS spectrum
1	243.2090	43.8	–	Fragment of DAG (18:2/18:2)	–
2	261.2182	43.8	–	Fragment of DAG (18:2/18:2)	–
3	263.2362	44.0	–	Fragment of DAG (16:0/18:2)	–
4	299.2571	44.2	–	Fragment of DAG (16:0/18:2)	–
5	331.2789	44.0	–	Fragment of DAG (16:0/18:2)	–
6	337.2740	44.0	–	Fragment of DAG (16:0/18:2)	–
7	339.2896	44.6	–	Fragment of DAG (18:2/20:2)	–
8	357.2972	44.4	–	Fragment of DAG (18:1/18:2)	–
9	505.3885	43.8	–	Fragment of DAG (18:2/18:2) (?)	–
10	577.5185	44.6	$[M - H_2O + H]^+$	DAG (16:0/18:1)	–
11	593.5154	44.1	$[M + H]^+$	DAG (16:0/18:2)	–
12	595.5281	44.6	$[M + H]^+$	DAG (16:0/18:1)	–
13	599.5026	43.8	$[M - H_2O + H]^+$	DAG (18:2/18:2)	–
14	601.5186	44.4	$[M - H_2O + H]^+$	DAG (18:1/18:2)	–
15	603.5334	44.9	$[M - H_2O + H]^+$	DAG (18:1/18:1)	–
16	605.5484	44.0	$[M - H_2O + C_2H_6 + H]^+$	DAG (16:0/18:2)	–
17	617.5133	43.7	$[M + H]^+$	DAG (18:2/18:2)	–
18	617.5101	44.7	$[M - H_2 + H]^+$	DAG (18:1/18:2)	–
19	619.5266	44.4	$[M + H]^+$	DAG (18:1/18:2)	–
20	621.5416	44.9	$[M + H]^+$	DAG (18:1/18:1)	–
21	631.5539	44.2	$[M - H_2O + C_2H_6 + H_2 + H]^+$	DAG (18:2/18:2)	–
22	633.5441	44.6	$[M + CH_2 + H]^+$	DAG (18:1/18:2)	–
23	634.5394	43.8	$[M + NH_4]^+$	DAG (18:2/18:2)	SI, p. S8
24	636.5550	44.4	$[M + NH_4]^+$	DAG (18:1/18:2)	SI, p. S9
25	638.5700	44.9	$[M + NH_4]^+$	DAG (18:1/18:1)	SI, p. S10
26	639.4951	43.8	$[M + Na]^+$	DAG (18:2/18:2)	–
27	640.5815	45.3	$[M + NH_4]^+$	DAG (18:0/18:1)	SI, p. S11
28	641.5108	44.3	$[M + Na]^+$	DAG (18:1/18:2)	–
29	643.5256	44.9	$[M + Na]^+$	DAG (18:1/18:1)	–
30	645.5386	45.4	$[M + Na]^+$	DAG (18:0/18:1)	–
31	655.4700	43.7	$[M + K]^+$	DAG (18:2/18:2)	–
32	657.4889	44.3	$[M + K]^+$	DAG (18:1/18:2)	–
33	659.5346	44.9	$[M + K]^+$	DAG (18:1/18:1)	–
34	662.5667	44.6	$[M + NH_4]^+$	DAG (18:2/20:2)	SI, p. S12
35	664.6204	45.1	$[M + NH_4]^+$	DAG (18:2/20:1) and some DAG (18:1/20:2)	SI, p. S13
36	667.5271	44.6	$[M + Na]^+$	DAG (18:2/20:2)	–
37	816.7036	47.6	$[M + NH_4]^+$	TAG (12:0/18:2/18:2) and isomers	SI, p. S14
38	844.7360	47.8	$[M + NH_4]^+$	TAG (14:0/18:2/18:2) and isomers	SI, p. S15

(Continues)

TABLE A2: (Continued)

(a) Identified significantly elevated positive-mode ions in ethanol-treated intracellular *A. niger* samples (potential identification and MS/MS spectrum)

No.	*m/z*	RT (min)	Ion	Potential identification	MS/MS spectrum
39	860.7302	46.6	$[M + NH_4]^+$	hTAG (16:1/16:1(OH)/18:2) (?)	–
40	862.7455	46.9	$[M + NH_4]^+$	hTAG (16:0/16:1(OH)/18:2)	SI, p. S16
41	864.7565	47.2	$[M + NH_4]^+$	hTAG (16:0/16:0/18:2(OH))	SI, p. S17
42	879.7409	46.5	$[M + H]^+$	TAG (18:2/18:2/18:2)	–
43	886.7387	46.8	$[M + NH_4]^+$	hTAG (16:0/18:2(OH)/18:3) (?)	–
44	888.7606	47.1	$[M + NH_4]^+$	hTAG (16:0/18:2/18:2(OH))	SI, p. S18
45	890.7736	47.3	$[M + NH_4]^+$	hTAG (16:0/18:1/18:2(OH))	SI, p. S19
46	904.8319	49.0	$[M + NH_4]^+$	TAG (18:0/18:1/18:1)	SI, p. S20
47	906.8451	49.1	$[M + NH_4]^+$	TAG (18:0/18:0/18:1)	SI, p. S21
48	912.7626	46.9	$[M + NH_4]^+$	hTAG (18:1/18:2(OH)/18:3) and isomers	SI, p. S22
49	914.7771	47.2	$[M + NH_4]^+$	hTAG (18:1/18:2/18:2(OH))	SI, p. S23
50	916.7929	47.5	$[M + NH_4]^+$	hTAG (18:1/18:1/18:2(OH))	SI, p. S24
51	918.8068	47.7	$[M + NH_4]^+$	hTAG (18:0/18:1/18:2(OH))	SI, p. S25
52	934.8749	49.5	$[M + NH_4]^+$	TAG (18:0/18:1/20:0) and other isomers	SI, p. S26
53	990.9377	50.2	$[M + NH_4]^+$	TAG (18:0/18:1/24:0)	SI, p. S27
54	1,002.9375	50.2	$[M + NH_4]^+$	TAG (18:1/18:1/25:0)	SI, p. S28
55	1,004.9508	50.4	$[M + NH_4]^+$	TAG (18:0/18:1/25:0) (?)	–
56	1,018.9654	50.5	$[M + NH_4]^+$	TAG (18:0/18:1/26:0)	SI, p. S29
57	1,231.9962	43.8	$[2M - H_2 + H]^+$	DAG (18:2/18:2)	–
58	1,234.0106	44.1	$[2M + H]^+$	DAG (18:2/18:2) (?)	–
59	1,236.0261	44.3	$[2M - H_2 + H]^+$	DAG (18:1/18:2)	–
60	1,238.0424	44.8	$[M + H]^+$	DAG (18:1/18:1) + DAG (18:2/18:2)	–
61	1,255.9951	43.7	$[2M + Na]^+$	DAG (18:2/18:2)	–
62	1,260.0226	44.3	$[2M + Na]^+$	DAG (18:1/18:2)	–
63	1264.0575	45.0	$[2M + Na]^+$	DAG (18:1/18:1)	–

(b) Identified significantly elevated positive-mode ions in ethanol-treated intracellular *A. niger* samples (MSII)

NO.	*m/z*	RT (min)	Integrated mass ion intensity (MSII)							
			EtOH-1	EtOH-2	EtOH-3	EtOH-avg	Con-1	Con-2	Con-3	Con-avg
1	243.2090	43.8	6.14E+04	4.25E+04	4.54E+04	4.98E+04	1.68E+04	1.42E+04	1.86E+04	1.65E+04
2	261.2182	43.8	3.14E+05	2.07E+05	2.35E+05	2.52E+05	8.54E+04	6.46E+04	1.16E+05	8.86E+04
3	263.2362	44.0	9.81E+05	7.13E+05	8.18E+05	8.37E+05	3.26E+05	2.60E+05	4.16E+05	3.34E+05
4	299.2571	44.2	1.72E+04	2.82E+04	2.56E+04	2.37E+04	7.81E+03	8.39E+03	8.35E+03	8.18E+03
5	331.2789	44.0	1.87E+05	1.27E+05	1.54E+05	1.56E+05	7.13E+04	5.52E+04	9.16E+04	7.27E+04
6	337.2740	44.0	1.18E+07	8.40E+06	9.33E+06	9.86E+06	2.82E+06	2.33E+06	3.69E+06	2.95E+06
7	339.2896	44.6	1.09E+07	9.04E+06	9.03E+06	9.67E+06	2.18E+06	1.64E+06	2.92E+06	2.25E+06
8	357.2972	44.4	8.13E+04	6.16E+04	6.28E+04	6.86E+04	1.91E+04	1.51E+04	2.27E+04	1.89E+04
9	505.3885	43.8	6.89E+04	3.99E+04	4.40E+04	5.10E+04	1.32E+04	1.17E+04	1.58E+04	1.35E+04
10	577.5185	44.6	2.10E+06	1.80E+06	2.14E+06	2.02E+06	8.52E+05	6.66E+05	1.19E+06	9.04E+05
11	593.5154	44.1	3.19E+05	2.27E+05	2.70E+05	2.72E+05	1.25E+05	1.01E+05	1.56E+05	1.28E+05
12	595.5281	44.6	1.90E+05	1.73E+05	1.70E+05	1.78E+05	7.65E+04	6.12E+04	1.03E+05	8.01E+04

(Continues)

TABLE A2: (Continued)

(b) Identified significantly elevated positive-mode ions in ethanol-treated intracellular *A. niger* samples (MSII)

NO.	*m/z*	RT (min)	Integrated mass ion intensity (MSII)							
			EtOH-1	EtOH-2	EtOH-3	EtOH-avg	Con-1	Con-2	Con-3	Con-avg
13	599.5026	43.8	2.80E+06	1.70E+06	1.90E+06	2.13E+06	5.39E+05	4.38E+05	5.83E+05	5.20E+05
14	601.5186	44.4	4.16E+06	3.46E+06	3.26E+06	3.63E+06	9.62E+05	7.49E+05	1.16E+06	9.58E+05
15	603.5334	44.9	3.49E+06	3.09E+06	2.97E+06	3.18E+06	8.51E+05	6.37E+05	9.90E+05	8.26E+05
16	605.5484	44.0	8.82E+05	9.92E+05	1.22E+06	1.03E+06	0.00E+00	3.30E+05	3.98E+05	2.42E+05
17	617.5133	43.7	6.33E+06	3.80E+06	4.06E+06	4.73E+06	1.14E+06	9.60E+05	1.34E+06	1.15E+06
18	617.5101	44.7	5.45E+04	7.25E+04	1.01E+05	7.59E+04	4.26E+04	2.30E+04	3.19E+04	3.25E+04
19	619.5266	44.4	2.09E+06	1.66E+06	1.57E+06	1.77E+06	4.97E+05	3.95E+05	6.40E+05	5.11E+05
20	621.5416	44.9	5.78E+05	5.25E+05	4.47E+05	5.17E+05	1.34E+05	1.05E+05	1.84E+05	1.41E+05
21	631.5539	44.2	5.90E+04	6.91E+04	8.55E+04	7.12E+04	0.00E+00	0.00E+00	1.34E+03	4.47E+02
22	633.5441	44.6	1.14E+04	2.51E+04	2.37E+04	2.01E+04	0.00E+00	4.73E+03	5.80E+03	3.51E+03
23	634.5394	43.8	3.66E+06	2.28E+06	2.11E+06	2.68E+06	7.41E+05	5.42E+05	7.47E+05	6.77E+05
24	636.5550	44.4	2.82E+06	2.21E+06	1.89E+06	2.30E+06	6.98E+05	4.98E+05	7.58E+05	6.51E+05
25	638.5700	44.9	2.01E+06	1.78E+06	1.49E+06	1.76E+06	5.18E+05	3.72E+05	5.97E+05	4.96E+05
26	639.4951	43.8	1.03E+06	7.02E+05	8.05E+05	8.45E+05	1.82E+05	1.16E+05	2.06E+05	1.68E+05
27	640.5815	45.3	6.84E+05	6.19E+05	4.95E+05	5.99E+05	1.32E+05	1.02E+05	1.54E+05	1.29E+05
28	641.5108	44.3	7.54E+05	7.40E+05	8.55E+05	7.83E+05	2.20E+05	1.42E+05	2.41E+05	2.01E+05
29	643.5256	44.9	5.60E+05	6.48E+05	6.90E+05	6.33E+05	2.65E+05	1.51E+05	2.12E+05	2.09E+05
30	645.5386	45.4	2.36E+05	3.23E+05	3.02E+05	2.87E+05	9.56E+04	6.22E+04	6.83E+04	7.53E+04
31	655.4700	43.7	3.34E+04	2.28E+04	2.56E+04	2.73E+04	7.36E+03	6.12E+03	7.46E+03	6.98E+03
32	657.4889	44.3	2.75E+04	2.54E+04	2.73E+04	2.67E+04	1.10E+04	7.86E+03	1.09E+04	9.90E+03
33	659.5346	44.9	5.13E+04	3.76E+04	4.59E+04	4.49E+04	1.48E+04	6.56E+03	9.97E+03	1.05E+04
34	662.5667	44.6	9.14E+04	7.21E+04	5.92E+04	7.42E+04	1.87E+04	1.33E+04	2.06E+04	1.75E+04
35	664.6204	45.1	7.79E+04	6.74E+04	5.29E+04	6.61E+04	1.70E+04	1.54E+04	2.07E+04	1.77E+04
36	667.5271	44.6	2.50E+04	2.23E+04	2.28E+04	2.34E+04	7.71E+03	2.65E+03	3.69E+03	4.68E+03
37	816.7036	47.6	1.89E+05	1.63E+05	1.50E+05	1.68E+05	4.36E+04	3.54E+04	3.32E+04	3.74E+04
38	844.7360	47.8	1.24E+06	1.11E+06	1.04E+06	1.13E+06	5.17E+05	4.83E+05	4.51E+05	4.84E+05
39	860.7302	46.6	4.87E+04	3.27E+04	3.70E+04	3.94E+04	2.95E+03	3.49E+03	5.87E+03	4.10E+03
40	862.7455	46.9	1.11E+05	8.84E+04	1.09E+05	1.03E+05	3.89E+04	3.38E+04	5.26E+04	4.18E+04
41	864.7565	47.2	1.13E+05	1.06E+05	1.06E+05	1.08E+05	4.50E+04	4.77E+04	5.22E+04	4.83E+04
42	879.7409	46.5	3.85E+05	2.77E+05	3.44E+05	3.35E+05	0.00E+00	6.04E+04	5.62E+04	3.89E+04
43	886.7387	46.8	4.56E+05	3.16E+05	4.05E+05	3.92E+05	1.89E+05	9.46E+04	1.17E+05	1.34E+05
44	888.7606	47.1	6.34E+05	4.53E+05	5.12E+05	5.33E+05	1.27E+05	9.66E+04	1.45E+05	1.23E+05
45	890.7736	47.3	5.16E+05	4.09E+05	4.70E+05	4.65E+05	1.84E+05	1.46E+05	1.58E+05	1.63E+05
46	904.8319	49.0	1.20E+07	1.17E+07	1.12E+07	1.16E+07	5.20E+06	5.14E+06	4.32E+06	4.89E+06
47	906.8451	49.1	6.89E+06	6.87E+06	6.62E+06	6.79E+06	2.54E+06	2.70E+06	1.83E+06	2.36E+06
48	912.7626	46.9	6.04E+05	3.94E+05	4.14E+05	4.71E+05	8.59E+04	7.87E+04	7.21E+04	7.89E+04
49	914.7771	47.2	7.27E+05	5.06E+05	5.55E+05	5.96E+05	9.83E+04	9.24E+04	9.40E+04	9.49E+04
50	916.7929	47.5	5.63E+05	4.16E+05	4.71E+05	4.84E+05	7.59E+04	6.54E+04	1.68E+05	1.03E+05
51	918.8068	47.7	2.68E+05	2.07E+05	2.53E+05	2.43E+05	4.88E+04	4.53E+04	4.49E+04	4.63E+04
52	934.8749	49.5	9.33E+05	1.02E+06	9.33E+05	9.62E+05	4.54E+05	4.52E+05	3.34E+05	4.13E+05
53	990.9377	50.2	4.77E+06	4.56E+06	4.16E+06	4.50E+06	2.04E+06	2.45E+06	1.71E+06	2.07E+06
54	1,002.9375	50.2	8.96E+05	8.10E+05	7.02E+05	8.02E+05	3.15E+05	3.43E+05	2.54E+05	3.04E+05
55	1,004.9508	50.4	7.08E+05	6.30E+05	5.66E+05	6.34E+05	1.78E+05	1.91E+05	1.33E+05	1.67E+05

(Continues)

TABLE A2: (Continued)

(b) Identified significantly elevated positive-mode ions in ethanol-treated intracellular *A. niger* samples (MSII)

NO.	*m/z*	RT (min)	Integrated mass ion intensity (MSII)							
			EtOH-1	EtOH-2	EtOH-3	EtOH-avg	Con-1	Con-2	Con-3	Con-avg
56	1,018.9654	50.5	7.98E+05	7.61E+05	6.96E+05	7.52E+05	2.94E+05	3.54E+05	2.54E+05	3.01E+05
57	1,231.9962	43.8	2.92E+04	2.23E+04	2.21E+04	2.45E+04	9.12E+03	5.33E+03	9.03E+03	7.83E+03
58	1,234.0106	44.1	4.12E+04	3.93E+04	3.15E+04	3.73E+04	1.59E+04	9.40E+03	1.51E+04	1.35E+04
59	1,236.0261	44.3	4.62E+04	4.30E+04	3.95E+04	4.29E+04	1.65E+04	1.09E+04	1.74E+04	1.49E+04
60	1,238.0424	44.8	5.91E+04	6.23E+04	5.54E+04	5.89E+04	2.47E+04	1.28E+04	2.30E+04	2.02E+04
61	1,255.9951	43.7	4.14E+04	3.05E+04	2.37E+04	3.19E+04	6.23E+03	3.47E+03	5.24E+03	4.98E+03
62	1,260.0226	44.3	4.14E+04	4.31E+04	3.21E+04	3.89E+04	1.00E+04	6.42E+03	9.24E+03	8.56E+03
63	1,264.0575	45.0	8.14E+04	9.04E+04	6.78E+04	7.99E+04	2.49E+04	1.43E+04	2.03E+04	1.98E+04

(c) Identified significantly elevated positive-mode ions in ethanol-treated intracellular *A. niger* samples (aMSII)

No.	*m/z*	RT (min)	Adjusted integrated mass ion intensity (aMSII)							
			EtOH-1	EtOH-2	EtOH-3	EtOH-avg	Con-1	Con-2	Con-3	Con-avg
1	243.2090	43.8	8.85E+04	6.12E+04	6.54E+04	7.17E+04	1.29E+04	1.09E+04	1.42E+04	1.27E+04
2	261.2182	43.8	4.52E+05	2.99E+05	3.39E+05	3.63E+05	6.54E+04	4.95E+04	8.86E+04	6.78E+04
3	263.2362	44.0	1.41E+06	1.03E+06	1.18E+06	1.21E+06	2.50E+05	1.99E+05	3.18E+05	2.56E+05
4	299.2571	44.2	2.47E+04	4.07E+04	3.68E+04	3.41E+04	5.98E+03	6.42E+03	6.39E+03	6.27E+03
5	331.2789	44.0	2.70E+05	1.83E+05	2.22E+05	2.25E+05	5.46E+04	4.23E+04	7.02E+04	5.57E+04
6	337.2740	44.0	1.71E+07	1.21E+07	1.34E+07	1.42E+07	2.16E+06	1.78E+06	2.83E+06	2.26E+06
7	339.2896	44.6	1.58E+07	1.30E+07	1.30E+07	1.39E+07	1.67E+06	1.25E+06	2.23E+06	1.72E+06
8	357.2972	44.4	1.17E+05	8.87E+04	9.04E+04	9.87E+04	1.46E+04	1.15E+04	1.74E+04	1.45E+04
9	505.3885	43.8	9.92E+04	5.75E+04	6.34E+04	7.34E+04	1.01E+04	8.93E+03	1.21E+04	1.04E+04
10	577.5185	44.6	3.03E+06	2.60E+06	3.08E+06	2.90E+06	6.53E+05	5.10E+05	9.14E+05	6.92E+05
11	593.5154	44.1	4.59E+05	3.27E+05	3.89E+05	3.92E+05	9.60E+04	7.73E+04	1.20E+05	9.77E+04
12	595.5281	44.6	2.73E+05	2.49E+05	2.45E+05	2.56E+05	5.86E+04	4.69E+04	7.86E+04	6.14E+04
13	599.5026	43.8	4.04E+06	2.45E+06	2.74E+06	3.07E+06	4.13E+05	3.35E+05	4.46E+05	3.98E+05
14	601.5186	44.4	5.99E+06	4.98E+06	4.70E+06	5.22E+06	7.37E+05	5.74E+05	8.92E+05	7.34E+05
15	603.5334	44.9	5.03E+06	4.45E+06	4.28E+06	4.59E+06	6.52E+05	4.88E+05	7.58E+05	6.33E+05
16	605.5484	44.0	1.27E+06	1.43E+06	1.76E+06	1.49E+06	0.00E+00	2.52E+05	3.05E+05	1.86E+05
17	617.5133	43.7	9.12E+06	5.47E+06	5.85E+06	6.81E+06	8.77E+05	7.35E+05	1.03E+06	8.79E+05
18	617.5101	44.7	7.85E+04	1.04E+05	1.45E+05	1.09E+05	3.26E+04	1.76E+04	2.44E+04	2.49E+04
19	619.5266	44.4	3.00E+06	2.39E+06	2.26E+06	2.55E+06	3.81E+05	3.03E+05	4.90E+05	3.91E+05
20	621.5416	44.9	8.32E+05	7.56E+05	6.44E+05	7.44E+05	1.03E+05	8.02E+04	1.41E+05	1.08E+05
21	631.5539	44.2	8.49E+04	9.96E+04	1.23E+05	1.03E+05	0.00E+00	0.00E+00	1.03E+03	3.43E+02
22	633.5441	44.6	1.64E+04	3.62E+04	3.42E+04	2.89E+04	0.00E+00	3.62E+03	4.44E+03	2.69E+03
23	634.5394	43.8	5.27E+06	3.28E+06	3.04E+06	3.86E+06	5.67E+05	4.15E+05	5.72E+05	5.18E+05
24	636.5550	44.4	4.06E+06	3.18E+06	2.73E+06	3.32E+06	5.34E+05	3.82E+05	5.81E+05	4.99E+05
25	638.5700	44.9	2.89E+06	2.56E+06	2.15E+06	2.53E+06	3.97E+05	2.85E+05	4.58E+05	3.80E+05
26	639.4951	43.8	1.48E+06	1.01E+06	1.16E+06	1.22E+06	1.40E+05	8.91E+04	1.57E+05	1.29E+05
27	640.5815	45.3	9.84E+05	8.91E+05	7.12E+05	8.62E+05	1.01E+05	7.84E+04	1.18E+05	9.92E+04
28	641.5108	44.3	1.09E+06	1.07E+06	1.23E+06	1.13E+06	1.69E+05	1.09E+05	1.85E+05	1.54E+05
29	643.5256	44.9	8.07E+05	9.34E+05	9.94E+05	9.11E+05	2.03E+05	1.16E+05	1.63E+05	1.60E+05
30	645.5386	45.4	3.39E+05	4.65E+05	4.35E+05	4.13E+05	7.32E+04	4.77E+04	5.23E+04	5.77E+04
31	655.4700	43.7	4.81E+04	3.28E+04	3.69E+04	3.93E+04	5.63E+03	4.69E+03	5.71E+03	5.35E+03
32	657.4889	44.3	3.96E+04	3.66E+04	3.93E+04	3.85E+04	8.40E+03	6.02E+03	8.33E+03	7.58E+03
33	659.5346	44.9	7.39E+04	5.41E+04	6.60E+04	6.47E+04	1.14E+04	5.02E+03	7.63E+03	8.01E+03

(Continues)

TABLE A2: (Continued)

(c) Identified significantly elevated positive-mode ions in ethanol-treated intracellular *A. niger* samples (aMSII)										
			Adjusted integrated mass ion intensity (aMSII)							
No.	*m/z*	RT (min)	EtOH-1	EtOH-2	EtOH-3	EtOH-avg	Con-1	Con-2	Con-3	Con-avg
34	662.5667	44.6	1.32E+05	1.04E+05	8.53E+04	1.07E+05	1.43E+04	1.02E+04	1.58E+04	1.34E+04
35	664.6204	45.1	1.12E+05	9.71E+04	7.62E+04	9.51E+04	1.31E+04	1.18E+04	1.59E+04	1.36E+04
36	667.5271	44.6	3.60E+04	3.21E+04	3.29E+04	3.37E+04	5.91E+03	2.03E+03	2.83E+03	3.59E+03
37	816.7036	47.6	2.72E+05	2.35E+05	2.16E+05	2.41E+05	3.34E+04	2.71E+04	2.54E+04	2.86E+04
38	844.7360	47.8	1.79E+06	1.60E+06	1.50E+06	1.63E+06	3.96E+05	3.70E+05	3.45E+05	3.70E+05
39	860.7302	46.6	7.01E+04	4.70E+04	5.33E+04	5.68E+04	2.26E+03	2.67E+03	4.49E+03	3.14E+03
40	862.7455	46.9	1.60E+05	1.27E+05	1.58E+05	1.48E+05	2.98E+04	2.59E+04	4.03E+04	3.20E+04
41	864.7565	47.2	1.62E+05	1.53E+05	1.53E+05	1.56E+05	3.45E+04	3.66E+04	4.00E+04	3.70E+04
42	879.7409	46.5	5.55E+05	3.99E+05	4.95E+05	4.83E+05	0.00E+00	4.63E+04	4.30E+04	2.98E+04
43	886.7387	46.8	6.56E+05	4.55E+05	5.83E+05	5.65E+05	1.45E+05	7.24E+04	9.00E+04	1.02E+05
44	888.7606	47.1	9.14E+05	6.53E+05	7.37E+05	7.68E+05	9.74E+04	7.40E+04	1.11E+05	9.41E+04
45	890.7736	47.3	7.43E+05	5.89E+05	6.77E+05	6.70E+05	1.41E+05	1.12E+05	1.21E+05	1.25E+05
46	904.8319	49.0	1.72E+07	1.69E+07	1.61E+07	1.67E+07	3.98E+06	3.94E+06	3.31E+06	3.74E+06
47	906.8451	49.1	9.93E+06	9.89E+06	9.53E+06	9.78E+06	1.95E+06	2.07E+06	1.40E+06	1.81E+06
48	912.7626	46.9	8.70E+05	5.67E+05	5.97E+05	6.78E+05	6.58E+04	6.03E+04	5.52E+04	6.04E+04
49	914.7771	47.2	1.05E+06	7.29E+05	7.99E+05	8.58E+05	7.53E+04	7.08E+04	7.20E+04	7.27E+04
50	916.7929	47.5	8.11E+05	6.00E+05	6.79E+05	6.96E+05	5.81E+04	5.01E+04	1.29E+05	7.89E+04
51	918.8068	47.7	3.87E+05	2.99E+05	3.64E+05	3.50E+05	3.74E+04	3.47E+04	3.44E+04	3.55E+04
52	934.8749	49.5	1.34E+06	1.47E+06	1.34E+06	1.39E+06	3.47E+05	3.46E+05	2.56E+05	3.16E+05
53	990.9377	50.2	6.88E+06	6.56E+06	5.99E+06	6.48E+06	1.57E+06	1.88E+06	1.31E+06	1.59E+06
54	1,002.9375	50.2	1.29E+06	1.17E+06	1.01E+06	1.16E+06	2.41E+05	2.62E+05	1.95E+05	2.33E+05
55	1,004.9508	50.4	1.02E+06	9.07E+05	8.15E+05	9.14E+05	1.36E+05	1.46E+05	1.02E+05	1.28E+05
56	1,018.9654	50.5	1.15E+06	1.10E+06	1.00E+06	1.08E+06	2.25E+05	2.71E+05	1.95E+05	2.30E+05
57	1,231.9962	43.8	4.20E+04	3.21E+04	3.18E+04	3.53E+04	6.98E+03	4.08E+03	6.92E+03	5.99E+03
58	1,234.0106	44.1	5.93E+04	5.65E+04	4.53E+04	5.37E+04	1.22E+04	7.20E+03	1.15E+04	1.03E+04
59	1,236.0261	44.3	6.65E+04	6.19E+04	5.69E+04	6.18E+04	1.26E+04	8.33E+03	1.33E+04	1.14E+04
60	1,238.0424	44.8	8.50E+04	8.97E+04	7.97E+04	8.48E+04	1.89E+04	9.81E+03	1.76E+04	1.54E+04
61	1,255.9951	43.7	5.97E+04	4.39E+04	3.42E+04	4.59E+04	4.77E+03	2.66E+03	4.01E+03	3.81E+03
62	1,260.0226	44.3	5.97E+04	6.20E+04	4.62E+04	5.60E+04	7.68E+03	4.92E+03	7.08E+03	6.56E+03
63	1,264.0575	45.0	1.17E+05	1.30E+05	9.77E+04	1.15E+05	1.91E+04	1.09E+04	1.55E+04	1.52E+04

TABLE A3: Other lipids in the pathways found in intracellular *A. niger* samples. Lipids are shown in terms of their lipid class and acyl chain as (a) detected ion adduct, measured mass-to-charge ratio (*m/z*), retention time (RT), MS/MS spectrum, (b) integrated mass ion intensity (MSII) and (c) adjusted mass ion intensity (aMSII). The MSII and aMSII data are shown for three *A. niger* samples without (Con-1–3) or with ethanol treatments (EtOH-1–3) and their respective averages (Con-avg and EtOH-avg, respectively)

(a) Other intracellular lipids in the pathways (ion, *m/z*, RT, MS/MS spectrum)					
	Lipid class				
No.	Acyl chain	Ions	*m/z*	RT (min)	MS/MS spectrum
	Fatty acid (FA)				
1	16:0	$[M-H]^-$	255.2317	18.6	–
2	18:2	$[M-H]^-$	279.2336	18.5	–
3	18:1	$[M-H]^-$	281.2478	18.8	–
4	18:0	$[M-H]^-$	283.2624	19.2	–
	Monoacylglycerol (MAG)				

(Continues)

TABLE A3: (Continued)

(a) Other intracellular lipids in the pathways (ion, *m/z*, RT, MS/MS spectrum)

No.	Lipid class: Acyl chain	Ions	*m/z*	RT (min)	MS/MS spectrum
3	16:0	$[M + Na]^+$	353.2656	34.0	–
4	18:2	$[M + Na]^+$	377.2718	33.1	–
	Phosphatidic acid (PA)				
5	16:0/18:2	$[M - H]^-$	671.4649	27.4	SI, p. S32
6	18:2/18:2	$[M - H]^-$	695.4647	26.8	SI, p. S33
	Phosphatidylethanolamine (PE)				
7	16:0/18:2	$[M - H]^-$	714.5023	39.0	SI, p. S34
8	18:2/18:2	$[M - H]^-$	738.5004	38.2	SI, p. S35
	Phosphatidylserine (PS)				
9	16:0/18:2	$[M - H]^-$	758.4944	29.9	SI, p. S36
10	18:2/18:2	$[M - H]^-$	782.4946	29.3	SI, p. S37
	Phosphatidylglycerol (PG)				
11	16:0/18:2	$[M - H]^-$	745.4976	34.4	SI, p. S38
12	18:2/18:2	$[M - H]^-$	769.4962	33.8	SI, p. S39
	Phosphatidylinositol (PI)				
13	16:0/18:2	$[M - H]^-$	833.5160	34.0	SI, p. S40
14	18:2/18:2	$[M - H]^-$	857.5147	33.4	SI, p. S41
	Phosphatidylcholine (PC)				
15	16:0/18:2	$[M + H]^+$	758.5726	41.7	SI, p. S30
16	18:2/18:2	$[M + H]^+$	782.5751	41.3	SI, p. S31

(b) Other intracellular lipids in the pathways (MSII)

No.	Lipid class: Acyl chain	Integrated mass ion intensity (MSII): EtOH-1	EtOH-2	EtOH-3	EtOH-avg	Con-1	Con-2	Con-3	Con-avg
	Fatty acid (FA)								
1	16:0	2.26E+06	2.16E+06	1.99E+06	2.14E+06	2.43E+06	2.48E+06	2.53E+06	2.48E+06
2	18:2	1.48E+07	1.31E+07	1.38E+07	1.39E+07	1.56E+07	1.57E+07	1.57E+07	1.57E+07
3	18:1	7.86E+06	7.31E+06	6.94E+06	7.37E+06	7.03E+06	6.66E+06	7.33E+06	7.01E+06
4	18:0	1.51E+06	1.47E+06	1.36E+06	1.44E+06	1.91E+06	1.73E+06	1.77E+06	1.80E+06
	Monoacylglycerol (MAG)								
3	16:0	5.15E+05	4.80E+05	3.36E+05	4.44E+05	3.23E+05	5.30E+05	4.54E+05	4.36E+05
4	18:2	3.46E+05	1.88E+05	2.70E+05	2.68E+05	3.21E+05	3.07E+05	2.98E+05	3.09E+05
	Phosphatidic acid (PA)								
5	16:0/18:2	9.63E+05	1.32E+06	7.26E+05	1.00E+06	1.34E+06	1.18E+06	9.63E+05	1.16E+06
6	18:2/18:2	1.03E+06	1.47E+06	1.08E+06	1.20E+06	9.08E+05	1.04E+06	9.54E+05	9.68E+05
	Phosphatidylethanolamine (PE)								
7	16:0/18:2	3.62E+05	7.06E+05	4.47E+05	5.05E+05	1.03E+06	9.95E+05	8.92E+05	9.72E+05
8	18:2/18:2	2.77E+05	4.11E+05	3.38E+05	3.42E+05	3.80E+05	3.64E+05	3.75E+05	3.73E+05
	Phosphatidylserine (PS)								
9	16:0/18:2	1.08E+06	1.64E+06	1.35E+06	1.36E+06	2.30E+06	1.87E+06	1.64E+06	1.94E+06
10	18:2/18:2	3.07E+05	3.50E+05	4.30E+05	3.62E+05	4.76E+05	4.50E+05	4.35E+05	4.54E+05
	Phosphatidylglycerol (PG)								

(Continues)

TABLE A3: (Continued)

(b) Other intracellular lipids in the pathways (MSII)									
	Lipid class	Integrated mass ion intensity (MSII)							
No.	Acyl chain	EtOH-1	EtOH-2	EtOH-3	EtOH-avg	Con-1	Con-2	Con-3	Con-avg
11	16:0/18:2	1.03E+05	1.59E+05	1.11E+05	1.24E+05	1.89E+05	1.75E+05	1.49E+05	1.71E+05
12	18:2/18:2	2.22E+04	4.09E+04	2.56E+04	2.96E+04	4.18E+04	3.44E+04	3.51E+04	3.71E+04
	Phosphatidylinositol (PI)								
13	16:0/18:2	9.00E+05	1.20E+06	9.51E+05	1.02E+06	1.73E+06	1.65E+06	1.37E+06	1.59E+06
14	18:2/18:2	4.21E+05	5.89E+05	4.83E+05	4.98E+05	9.33E+05	8.45E+05	8.03E+05	8.60E+05
	Phosphatidylcholine (PC)								
15	16:0/18:2	4.97E+06	5.26E+06	4.69E+06	4.97E+06	1.21E+07	1.22E+07	1.10E+07	1.18E+07
16	18:2/18:2	2.06E+07	2.15E+07	2.00E+07	2.07E+07	2.25E+07	2.26E+07	2.13E+07	2.22E+07

(c) Other intracellular lipids in the pathways (aMSII)									
	Lipid class	Adjusted integrated mass ion intensity (aMSII)							
No.	Acyl chain	EtOH-1	EtOH-2	EtOH-3	EtOH-avg	Con-1	Con-2	Con-3	Con-avg
	Fatty acid (FA)								
1	16:0	3.25E+06	3.11E+06	2.87E+06	3.08E+06	1.86E+06	1.90E+06	1.94E+06	1.90E+06
2	18:2	2.14E+07	1.89E+07	1.99E+07	2.01E+07	1.20E+07	1.20E+07	1.20E+07	1.20E+07
3	18:1	1.13E+07	1.05E+07	1.00E+07	1.06E+07	5.39E+06	5.10E+06	5.62E+06	5.37E+06
4	18:0	2.17E+06	2.11E+06	1.95E+06	2.08E+06	1.46E+06	1.33E+06	1.36E+06	1.38E+06
	Monoacylglycerol (MAG)								
3	16:0	8.76E+05	8.16E+05	5.71E+05	7.54E+05	2.29E+05	3.76E+05	3.22E+05	3.09E+05
4	18:2	5.88E+05	3.19E+05	4.58E+05	4.55E+05	2.27E+05	2.17E+05	2.11E+05	2.19E+05
	Phosphatidic acid (PA)								
5	16:0/18:2	1.39E+06	1.91E+06	1.05E+06	1.45E+06	1.03E+06	9.02E+05	7.37E+05	8.88E+05
6	18:2/18:2	1.49E+06	2.12E+06	1.56E+06	1.72E+06	6.95E+05	7.98E+05	7.30E+05	7.41E+05
	Phosphatidylethanolamine (PE)								
7	16:0/18:2	5.21E+05	1.02E+06	6.44E+05	7.27E+05	7.89E+05	7.62E+05	6.83E+05	7.45E+05
8	18:2/18:2	4.00E+05	5.91E+05	4.86E+05	4.92E+05	2.91E+05	2.79E+05	2.87E+05	2.86E+05
	Phosphatidylserine (PS)								
9	16:0/18:2	1.56E+06	2.36E+06	1.94E+06	1.95E+06	1.76E+06	1.43E+06	1.26E+06	1.48E+06
10	18:2/18:2	4.42E+05	5.05E+05	6.19E+05	5.22E+05	3.65E+05	3.45E+05	3.33E+05	3.48E+05
	Phosphatidylglycerol (PG)								
11	16:0/18:2	1.48E+05	2.29E+05	1.59E+05	1.79E+05	1.45E+05	1.34E+05	1.14E+05	1.31E+05
12	18:2/18:2	3.19E+04	5.89E+04	3.69E+04	4.26E+04	3.20E+04	2.64E+04	2.69E+04	2.84E+04
	Phosphatidylinositol (PI)								
13	16:0/18:2	1.30E+06	1.73E+06	1.37E+06	1.46E+06	1.33E+06	1.26E+06	1.05E+06	1.21E+06
14	18:2/18:2	6.06E+05	8.48E+05	6.95E+05	7.17E+05	7.15E+05	6.47E+05	6.15E+05	6.59E+05
	Phosphatidylcholine (PC)								
15	16:0/18:2	7.16E+06	7.57E+06	6.76E+06	7.16E+06	9.24E+06	9.38E+06	8.41E+06	9.01E+06
16	18:2/18:2	2.96E+07	3.10E+07	2.88E+07	2.98E+07	1.73E+07	1.73E+07	1.63E+07	1.70E+07

APPENDIX 2:

Calculation and predicted isotopic patterns on the mass spectra of representative ions in the ethanol-d_6 samples when taking into account only deuterium exchanges of all hydrogens on the representative ions and natural abundances of elements.

BASE CALCULATION

As ethanol-d_6 (or CD_3CD_2OD) was added to the culture at the concentration of 4% (*v*/*v*), the medium had the following ratios of H_2O to CD_3CD_2OD:

By volume	96: 4
By mass (At 25°C, density of H_2O = 0.99707 g/ml and of ethanol = 0.78522 g/ml)	95.7: 3.1
By mole (MW of H_2O = 18.01528 g/mol and of CD_3CD_2OD = 52.10541 g/mol)	5.3: 0.060

Since H_2O has 2 protons, while CD_3CD_2OD has 1 deuteron, the mole ratio of proton (and some deuteron from water) to deuteron (from ethanol-d_6) is equal to 10.6: 0.060. However, considering that natural abundances of hydrogen and deuterium are 99.9844% and 0.0156%, respectively, the mole ratio of proton to deuteron then becomes 10.6: 0.062, which is equal to 100: 0.58.

(A) DIACYLGLYCEROL (DAG) (18:2/18:2)

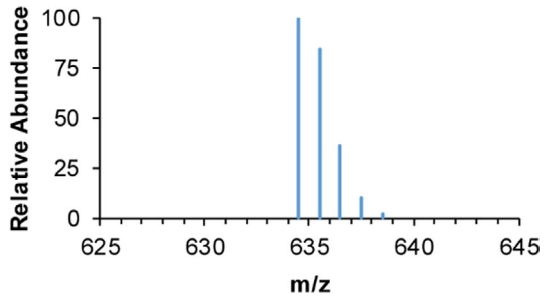

CALCULATION

$[M + NH_4]^+$ has the molecular formula of $C_{39}H_{72}NO_5^+$.

The highest probability of each isotope when considering only deuterium exchanges and natural isotopic abundance of each element is then equal to the following:

(Note: Terms with relatively small contribution are ignored below.)

$$M:\quad P(M)=P(0D)$$
$$={}^{72}C_0\left(\frac{0.58}{100}\right)^0\left(\frac{100}{100}\right)^{72}$$
$$=1.00$$

$$M+1:\quad P(M+1)=P(1D)+P\left(1^{13}C\right)$$
$$={}^{72}C_1\left(\frac{0.58}{100}\right)^1\left(\frac{100}{100}\right)^{71}+{}^{39}C_1\left(\frac{1.08}{100}\right)^1\left(\frac{100}{100}\right)^{38}$$
$$=0.84$$

$$M+2:\quad P(M+2)=P(2D)+P\left(2^{13}C\right)+P\left(1D\&1^{13}C\right)+P\left(1^{18}O\right)$$
$$={}^{72}C_2\left(\frac{0.58}{100}\right)^2\left(\frac{100}{100}\right)^{70}+{}^{39}C_2\left(\frac{1.08}{100}\right)^2\left(\frac{100}{100}\right)^{37}+P(1D)\cdot P\left(1^{13}C\right)+$$
$${}^{5}C_1\left(\frac{0.20}{100}\right)^1\left(\frac{100}{100}\right)^4$$
$$=0.36$$

$$M+3:\quad P(M+3)=P(3D)+P\left(3^{13}C\right)+P\left(2D\&1^{13}C\right)+P\left(1D\&2^{13}C\right)$$
$$+P\left(1D\&1^{18}O\right)+P\left(1^{13}C\&1^{18}O\right)$$
$$={}^{72}C_3\left(\frac{0.58}{100}\right)^3\left(\frac{100}{100}\right)^{69}+{}^{39}C_3\left(\frac{1.08}{100}\right)^3\left(\frac{100}{100}\right)^{36}$$
$$+P(2D)\cdot P\left(1^{13}C\right)$$
$$+P(1D)\cdot P\left(2^{13}C\right)+P(1D)\cdot P\left(1^{18}O\right)+P\left(1^{13}C\right)\cdot P\left(1^{18}O\right)$$
$$=0.10$$

$$M+4:\quad P(M+4)=P(4D)+P\left(4^{13}C\right)+P\left(3D\&1^{13}C\right)+P\left(2D\&2^{13}C\right)$$
$$+P\left(1D\&3^{13}C\right)+P\left(2D\&1^{18}O\right)+P\left(2^{13}C\&1^{18}O\right)$$
$$+P\left(1D\&1^{13}C+1^{18}O\right)={}^{72}C_4\left(\frac{0.58}{100}\right)^4\left(\frac{100}{100}\right)^{68}+{}^{39}C_4\left(\frac{1.08}{100}\right)^4\left(\frac{100}{100}\right)^{35}$$
$$+P(3D)\cdot P\left(1^{13}C\right)+P(2D)\cdot P\left(2^{13}C\right)+P(1D)\cdot P\left(3^{13}C\right)$$
$$+P(2D)\cdot P\left(1^{18}O\right)+P\left(2^{13}C\right)\cdot P\left(1^{18}O\right)$$
$$+P(1D)\cdot P\left(1^{13}C\right)\cdot P\left(1^{18}O\right)=0.02$$

Thus, *M*: *M* + 1: *M* + 2: *M* + 3: *M* + 4 = 100: 84: 36: 10: 2.

(B) TRIACYLGLYCEROL (TAG) (18:0/18:1/18:1)

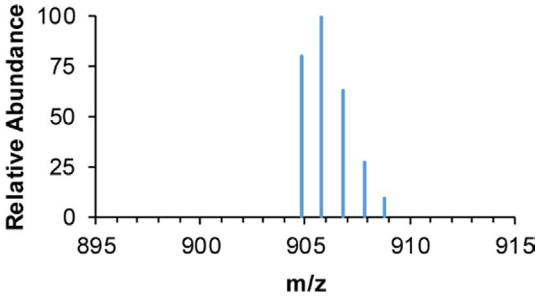

CALCULATION

$[M + NH_4]^+$ has the molecular formula of $C_{57}H_{110}NO_6^+$.

The highest probability of each isotope when considering only deuterium exchanges and natural isotopic abundance of each element is then equal to the following:

(Note: Terms with relatively small contribution are ignored below.)

$$M:\quad P(M)=P(0D)$$
$$={}^{110}C_0\left(\frac{0.58}{100}\right)^0\left(\frac{100}{100}\right)^{110}$$
$$=1.00$$

$$M+1:\quad P(M+1)=P(1D)+P\left(1^{13}C\right)$$
$$={}^{110}C_1\left(\frac{0.58}{100}\right)^1\left(\frac{100}{100}\right)^{109}+{}^{57}C_1\left(\frac{1.08}{100}\right)^1\left(\frac{100}{100}\right)^{56}$$
$$=1.26$$

$$M+2:\quad P(M+2)=P(2D)+P\left(2^{13}C\right)+P\left(1D\&1^{13}C\right)+P\left(1^{18}O\right)$$
$$={}^{110}C_2\left(\frac{0.58}{100}\right)^2\left(\frac{100}{100}\right)^{108}+{}^{57}C_2\left(\frac{1.08}{100}\right)^2\left(\frac{100}{100}\right)^{55}$$
$$+P(1D)\cdot P\left(1^{13}C\right)+{}^{6}C_1\left(\frac{0.20}{100}\right)^1\left(\frac{100}{100}\right)^5$$
$$=0.80$$

$$M+3:\quad P(M+3)=P(3D)+P\left(3^{13}C\right)+P\left(2D\&1^{13}C\right)$$
$$+P\left(1D\&2^{13}C\right)+P\left(1D\&1^{18}O\right)+P\left(1^{13}C\&1^{18}O\right)$$
$$={}^{110}C_3\left(\frac{0.58}{100}\right)^3\left(\frac{100}{100}\right)^{107}+{}^{57}C_3\left(\frac{1.08}{100}\right)^3\left(\frac{100}{100}\right)^{54}$$
$$+P(2D)\cdot P\left(1^{13}C\right)+P(1D)\cdot P\left(2^{13}C\right)+P(1D)\cdot P\left(1^{18}O\right)$$
$$+P\left(1^{13}C\right)\cdot P\left(1^{18}O\right)$$
$$=0.34$$

$$M+4:\quad P(M+4)=P(4D)+P\left(4^{13}C\right)+P\left(3D\&1^{13}C\right)$$
$$+P\left(2D\&2^{13}C\right)+P\left(1D\&3^{13}C\right)+P\left(2D\&1^{18}O\right)+P\left(2^{13}C\&1^{18}O\right)$$
$$+P\left(1D\&1^{13}C+1^{18}O\right)={}^{110}C_4\left(\frac{0.58}{100}\right)^4\left(\frac{100}{100}\right)^{106}$$
$$+{}^{57}C_4\left(\frac{1.08}{100}\right)^4\left(\frac{100}{100}\right)^{53}+P(3D)\cdot P\left(1^{13}C\right)+$$
$$P(2D)\cdot P\left(2^{13}C\right)+P(1D)\cdot P\left(3^{13}C\right)+P(2D)\cdot P\left(1^{18}O\right)+$$
$$P\left(2^{13}C\right)\cdot P\left(1^{18}O\right)+P(1D)\cdot P\left(1^{13}C\right)\cdot P\left(1^{18}O\right)$$
$$=0.11$$

Thus, M: $M+1$: $M+2$: $M+3$: $M+4$ = 80: 100: 63: 27: 9.

(C) FATTY ACID (FA) (18:2)

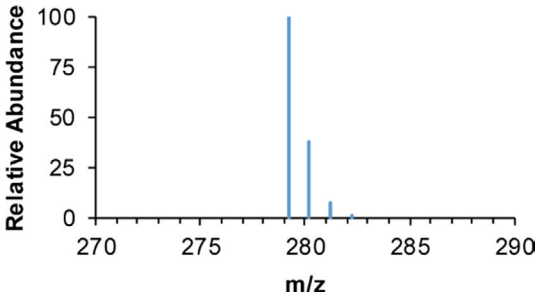

CALCULATION

$[M - H]^-$ has the molecular formula of $C_{18}H_{31}O_2^-$.

The highest probability of each isotope when considering only deuterium exchanges and natural isotopic abundance of each element is then equal to the following:

(Note: Terms with relatively small contribution are ignored below.)

$$M:\quad P(M)=P(0D)$$
$$={}^{31}C_0\left(\frac{0.58}{100}\right)^0\left(\frac{100}{100}\right)^{31}$$
$$=1.00$$

$$M+1:\quad P(M+1)=P(1D)+P\left(1^{13}C\right)$$
$$={}^{31}C_1\left(\frac{0.58}{100}\right)^1\left(\frac{100}{100}\right)^{30}+{}^{18}C_1\left(\frac{1.08}{100}\right)^1\left(\frac{100}{100}\right)^{17}$$
$$=0.38$$

$$M+2:\quad P(M+2)=P(2D)+P\left(2^{13}C\right)+P\left(1D\&1^{13}C\right)+$$
$$P\left(1^{18}O\right)={}^{31}C_2\left(\frac{0.58}{100}\right)^2\left(\frac{100}{100}\right)^{29}+{}^{18}C_2\left(\frac{1.08}{100}\right)^2\left(\frac{100}{100}\right)^{16}+$$
$$P(1D)\cdot P\left(1^{13}C\right)+{}^{2}C_1\left(\frac{0.20}{100}\right)^1\left(\frac{100}{100}\right)^1$$
$$=0.07$$

$$M+3:\quad P(M+3)=P(3D)+P\left(3^{13}C\right)+P\left(2D\&1^{13}C\right)+$$
$$P\left(1D\&2^{13}C\right)+P\left(1D\&1^{18}O\right)+P\left(1^{13}C\&1^{18}O\right)$$
$$={}^{31}C_3\left(\frac{0.58}{100}\right)^3\left(\frac{100}{100}\right)^{28}+{}^{18}C_3\left(\frac{1.08}{100}\right)^3\left(\frac{100}{100}\right)^{15}+$$
$$P(2D)\cdot P\left(1^{13}C\right)+P(1D)\cdot P\left(2^{13}C\right)+$$
$$P(1D)\cdot P\left(1^{18}O\right)+P\left(1^{13}C\right)\cdot P\left(1^{18}O\right)$$
$$=0.01$$

Thus, M: $M+1$: $M+2$: $M+3$ = 100: 38: 7: 1.

(D) PHOSPHATIDIC ACID (PA) (18:2/18:2)

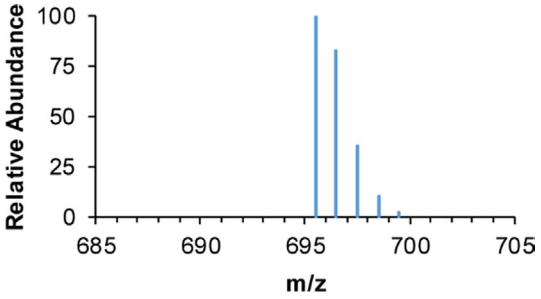

CALCULATION

$[M - H]^-$ has the molecular formula of $C_{39}H_{68}O_8P^-$.

The highest probability of each isotope when considering only deuterium exchanges and natural isotopic abundance of each element is then equal to the following:

(Note: Terms with relatively small contribution are ignored below.)

$$M:\quad P(M)=P(0D)$$
$$={}^{68}C_0\left(\frac{0.58}{100}\right)^0\left(\frac{100}{100}\right)^{68}$$
$$=1.00$$

$$M+1:\quad P(M+1)=P(1D)+P\left(1^{13}C\right)$$
$$={}^{68}C_1\left(\frac{0.58}{100}\right)^1\left(\frac{100}{100}\right)^{67}+{}^{39}C_1\left(\frac{1.08}{100}\right)^1\left(\frac{100}{100}\right)^{38}$$
$$=0.82$$

$$M+2:\quad P(M+2)=P(2D)+P\left(2^{13}C\right)+P\left(1D\&1^{13}C\right)+P\left(1^{18}O\right)$$
$$={}^{68}C_2\left(\frac{0.58}{100}\right)^2\left(\frac{100}{100}\right)^{66}+{}^{39}C_2\left(\frac{1.08}{100}\right)^2\left(\frac{100}{100}\right)^{37}+P(1D)\cdot P\left(1^{13}C\right)+$$
$${}^{8}C_1\left(\frac{0.20}{100}\right)^1\left(\frac{100}{100}\right)^{7}$$
$$=0.35$$

$$M+3:\quad P(M+3)=P(3D)+P\left(3^{13}C\right)+P\left(2D\&1^{13}C\right)+$$
$$P\left(1D\&2^{13}C\right)+P\left(1D\&1^{18}O\right)+P\left(1^{13}C\&1^{18}O\right)$$
$$={}^{68}C_3\left(\frac{0.58}{100}\right)^3\left(\frac{100}{100}\right)^{65}+{}^{39}C_3\left(\frac{1.08}{100}\right)^3\left(\frac{100}{100}\right)^{36}+$$
$$P(2D)\cdot P\left(1^{13}C\right)+P(1D)\cdot P\left(2^{13}C\right)+$$
$$P(1D)\cdot P\left(1^{18}O\right)+P\left(1^{13}C\right)\cdot P\left(1^{18}O\right)$$
$$=0.10$$

$$M+4:\quad P(M+4)=P(4D)+P\left(4^{13}C\right)+P\left(3D\&1^{13}C\right)+P\left(2D\&2^{13}C\right)+$$
$$P\left(1D\&3^{13}C\right)+P\left(2D\&1^{18}O\right)+P\left(2^{13}C\&1^{18}O\right)+$$
$$P\left(1D\&1^{13}C+1^{18}O\right)={}^{68}C_4\left(\frac{0.58}{100}\right)^4\left(\frac{100}{100}\right)^{64}+$$
$${}^{39}C_4\left(\frac{1.08}{100}\right)^4\left(\frac{100}{100}\right)^{35}+P(3D)\cdot P\left(1^{13}C\right)+$$
$$P(2D)\cdot P\left(2^{13}C\right)+P(1D)\cdot P\left(3^{13}C\right)+P(2D)\cdot P\left(1^{18}O\right)+$$
$$P\left(2^{13}C\right)\cdot P\left(1^{18}O\right)+P(1D)\cdot P\left(1^{13}C\right)\cdot P\left(1^{18}O\right)$$
$$=0.02$$

Thus, M: $M+1$: $M+2$: $M+3$: $M+4$ = 100: 82: 35: 10: 2.